RRB-87-03

For Submission to:

Water Resources Research

INTERPRETATION OF FIELD TRACER TESTS OF A SINGLE FRACTURE USING A TRANSIENT SOLUTE STORAGE MODEL

by
K.G. Raven[1], K.S. Novakowski[2]
and P.A. Lapcevic[2]

[1]National Hydrology Research Inst.
Environment Canada
Now at:
Intera Technologies Ltd.
1525 Carling Ave., Suite 600
Ottawa, Ontario K1Z 8R9

[2]National Water Research Institute
Environment Canada
867 Lakeshore Road
Burlington, Ontario L7R 4A6

NWRI Contribution #87-40

INTERPRETATION OF FIELD TRACER TESTS OF A SINGLE FRACTURE USING A TRANSIENT SOLUTE STORAGE MODEL

by

K.G. Raven[1]

National Hydrology Research Inst.

Environment Canada

562 Booth Street

Ottawa, Ontario, Canada K1A 0E7

K.S. Novakowski and P.A. Lapcevic

National Water Research Institute

867 Lakeshore Road

Burlington, Ontario, Canada L7R 4A6

[1]Now at:

Intera Technologies Ltd.

1525 Carling Ave., Suite 600

Ottawa, Ontario K1Z 8R9

For submission to:

Water Resources Research

MANAGEMENT PERSPECTIVE

This paper describes the results of several field experiments investigating hydrodynamic dispersion in a single rock fracture. This is a relatively new area of study in which there are very few documented field experiments particularily with the background information we have here. Consequently the results of this study have considerable importance in determining how we use groundwater transport models to predict the migration of contaminated groundwater away from waste sites overlying fractured rock. The Hyde Park Landfill and S-Area in Niagara Falls, NY are examples of such waste sites.

The results suggest that the well known advection-dispersion equation may be adequate for describing mass transport in a single fracture at natural rates of groundwater flow (i.e. our current advection-dispersion models may be suitable). Unfortunately, however, the fracture apertures determined from the tracer experiments do not agree with those obtained from the more commonly employed hydraulic test suggesting that the current conceptual model for predicting groundwater velocity in a single fracture may not be appropriate. These findings should be corroborated by conducting tracer experiments under more natural field conditions.

PERSPECTIVE - GESTION

Dans cet article, on présente les résultats d'expériences réalisées sur le terrain pour étudier la dispersion hydrodynamique dans une fracture unique. Comme ce champ d'étude est relativement nouveau, la documentation faisant état de ce genre d'expériences est pauvre, surtout si l'on cherche des cas où le travail est basé sur les mêmes données que celles qu'on a utilisées ici. Les résultats de cette étude revêtent donc une grande importance pour ceux qui utilisent des modèles sur le déplacement des eaux souterraines pour déterminer comment les eaux polluées migrent des installations d'élimination de déchets aménagées sur de la roche fracturée, ce qui est le cas, notamment, du site d'enfouissement sanitaire de Hyde Park et de la zone S à Niagara Falls (NY).

À en juger par les résultats qu'on a obtenus, l'équation d'advection-dispersion, qui est bien connue, serait indiquée pour décrire le déplacement de la masse d'eau souterraine dans une fracture unique en régime d'écoulement naturel (c'est-à-dire que nos modèles d'advection-dispersion actuels seraient adéquats). Malheureusement, les ouvertures repérées avec les traceurs ne concordent pas avec ce qu'on obtient par le test hydraulique plus communément employé, ce qui signifie que le modèle de conception qui s'emploie actuellement pour prévoir la vitesse d'écoulement des eaux souterraines dans une fracture unique ne serait pas correct. Il faudrait corroborer ces constatations en faisant des traçages dans des conditions plus naturelles.

ABSTRACT

The results and interpretation of five induced-gradient tracer tests performed at five different fluid velocities in a single fracture in monzonitic gneiss are described. The experiments were conducted using radioactive ^{82}Br and a fluorescent dye as conservative tracers where the tracers were pulse injected into radial-convergent and injection-withdrawal flow fields. The flow fields were established between straddle packers isolating the fracture in three boreholes over distances of 12.7-29.8 m. The tracer breakthrough curves were determined from samples of the withdrawn groundwater and were interpreted using residence time distribution (RTD) theory and two deterministic simulation models. The RTD curves of the tracer experiments were interpreted by fitting to the field data both a simple advection-dispersion model and an advection-dispersion model with transient solute storage in immobile fluid zones. Comparison of the fits obtained by the simulation models shows that the initial period of solute transport in single fractures is advection dominated and with increasing tracer residence time or decreasing fluid velocity, transport progresses towards more Fickian-like behaviour. During the advective-dominated period, the transient solute storage model is shown to adequately describe the asymmetries and long tails characteristic of the fracture RTDs. Interpretation of the tracer experiments using both simulation models indicate that induced-gradient tracer experiments are likely to underestimate the dispersive characteristics of single fractures under natural flow conditions.

RÉSUMÉ

On analyse les résultats de cinq traçages avec induction de gradient effectués à cinq régimes d'écoulement différents dans une fracture unique, dans du gneiss monzonitique. Pour faire les traçages on s'est servi de ^{82}Br radioactif et d'un colorant fluorescent, deux produits traceurs durables; on a injecté les traceurs en pulsations dans des champs d'écoulement de convergence radiale à injection avec soutirage. Ces champs se trouvaient entre les garnitures doubles qui isolaient la fracture dans trois trous de forage répartis sur des distances de 12,7 - 29,8 m. Pour tracer la courbe d'émergence des traceurs, on a analysé des échantillons tirés des eaux souterraines soutirées; on a analysé les courbes obtenues suivant la théorie de la distribution du temps de séjour (DTS), au moyen de deux modèles de simulation. Pour analyser les courbes de DTS tracées pour chaque expérience, on a comparé les données recueillies à un modèle d'advection et de dispersion simple et à un modèle d'advection et de dispersion avec rétention temporaire du soluté dans les zones de liquide immobile : on a constaté que le transport du soluté dans une fracture unique se fait d'abord surtout par advection et qu'à mesure que le séjour du traceur se prolonge ou que la vitesse d'écoulement diminue, il s'approche de plus en plus d'un mode de type Fickian. Durant la période où il se fait surtout par advection, le modèle à rétention temporaire représente bien les asymétries et les longues queues caractéristiques des DTS de la fracture. L'analyse réalisée au moyen des deux modèles de simulation montre qu'avec le traçage avec induction de gradient il est probable qu'on sous-estime la dispersion en écoulement naturel dans les fractures uniques.

INTRODUCTION

The prospect of storage and disposal of radioactive and toxic chemical wastes in fractured low-permeability geologic media has recently focussed attention on the fluid-flow and solute-transport properties of fractures. Understanding and quantifying the transport processes in single fractures is fundamental to the study and realistic prediction of solute migration in fracture-controlled groundwater flow systems.

The transport properties of single fractures are usually measured with tracer migration experiments at both laboratory and field scales. Such experiments are quite rare, particularly those performed at field scales under controlled conditions where the geometric and hydraulic properties of the fracture are well defined. Only recently have such field tracer experiments in fractures in low-permeability rock such as granite been reported in the literature (Klockars et al., 1982; Abelin et al., 1983; Hodgkinson and Lever, 1983; Novakowski et al., 1985a). In many of these field experiments as well as in laboratory studies with fractured granitic core (Neretnieks et al., 1982) the effluent tracer breakthrough curves often display a persistent skewness or tail that cannot be explained by a simple, one-dimensional Fickian-type model. Multiple flow domains (Klockars et al., 1982), diffusion and interaction of solute with the intact rock matrix (Neretnieks, 1983; Hodgkinson and Lever, 1983; Moreno et al., 1985) and discrete flow channelling (Neretnieks et al., 1982;

Moreno et al., 1985; Tsang and Tsang, 1987) have been proposed to account for the observed skewness.

There is a large body of experimental evidence and theoretical work from potentially analogous studies of one-dimensional dispersion in conduits (Taylor, 1953, 1954; Aris, 1956; Elder, 1959; Sayre, 1968; Gill and Sankarasubramanian, 1970; Chatwin, 1970; 1980), in rivers (Fisher, 1967; 1968) and in stratified aquifers (Gelhar et al., 1979; Matheron and de Marsily, 1980; Güven et al., 1984) that indicates Fickian-type behaviour only occurs after an initial advective-dominated period. During this advective-dominated period, the tracer concentration in the plane normal to flow is nonuniform, a sharply skewed distribution of tracer occurs in the direction of flow and calculated dispersion coefficients show a so-called scale effect (Fried, 1975; Pickens and Grisak, 1981) generally increasing with increasing travel distance or time. With increasing travel time, the influence of transverse mixing increases resulting in more uniform cross-sectional tracer concentrations, the distribution of tracer in the direction of flow approaches a Gaussian distribution and dispersion coefficients approach an assymptotic value characteristic of Fickian-type behaviour. Because of the limited number of reliable tracer experiments, it has not been possible to evaluate the applicability of the above concepts for studies of solute transport in single fractures. However, the observation that flow in single fractures is characterized by distinct and anastomosing flow channels (Maini, 1971) as a result of roughness and contact area effects (Iwai,

1976), intuitively suggests that analogues of flow in conduits, rivers and stratified aquifers are of practical use in the study of dispersion in single fractures.

The experimental observations from both conduit and river tracing studies (Aris, 1956; Fischer, 1968; Elhadi et al., 1984) indicate that one-dimensional non-Fickian behaviour can result from delayed or incomplete transverse mixing and suggests that a model which attempts to incorporate the processes of transverse mixing may be useful in interpreting highly-skewed tracer breakthrough curves. One model which accounts for the skewness observed in such studies more accurately than the Fickian-type advection-dispersion equation is the transient solute storage model or dead zone model (Turner, 1958; Aris, 1959; Coats and Smith, 1964). In this model, a term is included in the one-dimensional advection-dispersion equation to account for transverse solute mixing between mobile and immobile fluid phases. The immobile fluid phase is assumed to be stagnant relative to the longitudinal flow of the mobile fluid phase. The immobile fluid phase can occur as a consequence of irregularities in the cross section of the flow-through system (Thackston and Krenkel, 1970; Valentine and Wood, 1979) and from the existence of a laminar boundary layer (Taylor, 1954; Elder, 1959). In natural fractures, immobile zones or solute storage zones can be thought of as resulting from tortuous flow over and around large-scale roughness and asperities which protrude into and divide the flow path. Maini (1971) observed immobile fluid zones in plastic molds of natural fractures using dye experiments.

In this paper, the application of a transient solute storage model to analysis and interpretation of field tracer tests in a single fracture is presented. In addition, the concept of an initial advective-dominated period progressing to Fickian-type behaviour with increasing travel time as observed in analogous studies is evaluted for studies of solute transport in single fractures, by interpreting the results of five induced-gradient tracer tests performed at five different fluid velocities in the same fracture. These tracer tests are interpreted using both a simple advection-dispersion model and a transient solute storage model. Advection-dispersion models have previously been described and applied to field studies of transport in single fractures (Klockars et al., 1982; Neretnieks, 1982; Novakowski et al., 1985a). The governing equations and solutions of the transient solute storage model have previously been described and applied by numerous investigators in related studies (Coats and Smith, 1964; Hays, 1966; Thackston and Krenkel, 1967; Villermaux and Van Swaaij, 1969; Van Swaaij et al., 1969; Van Genuchten and Wierenga, 1976; 1977; Gaudet et al., 1977; Nordin and Troutman, 1980; Bencala and Walters, 1983; Black and Kipp, 1983; Legrand-Marcq and Laudelout, 1985). In this study, the solutions of the transient solute storage model are adapted for flow in a single fracture using the smooth parallel-plate model and are applied to the analysis and interpretation of tracer tests completed in radial-convergent and injection-withdrawal flow configurations.

The tracer experiments reported in this paper were performed over interborehole distances of 12.7-29.8 m between straddle packers isolating a single fracture in three boreholes in monzonitic gneiss at a depth of about 35 m. Radioactive, gamma-emitting ^{82}Br and Na Fluorescein (a fluorescent dye) were used as conservative tracers. The tracer experiments were designed to minimize and quantify the effect of mixing in the borehole instrumentation on the residence time distribution of tracer in the fracture.

SINGLE FRACTURE TRANSPORT MODELS

Advection-Dispersion (AD) Model

The most basic transport model which can be used to analyse the tracer experiments is the one-dimensional form of the well known advection-dispersion model. The equation is written as:

$$\frac{\partial C}{\partial t} = - \frac{v \partial C}{\partial x} + D_L \frac{\partial^2 C}{\partial x^2} \qquad (1)$$

where C is concentration, t is time, D_L is the longitudinal hydrodynamic dispersion coefficient in the direction of flow x, and v is average linear fluid velocity. For the time frames of the tracer experiments (<150 h), the longitudinal hydrodynamic dispersion coefficient is assumed to be dominated by mechanical mixing which is a linear function of average fluid velocity. This is written as $D_L = \alpha_L v$ where α_L is the longitudinal dispersivity. Systems which

exhibit transient concentration response described by equation (1) are said to show Fickian behaviour or to have reached the Taylor limit.

During the tracer experiments, tracer was instantaneously injected as a pulse. This can be expressed mathematically as a Dirac impulse function $\delta(x - x')$, where $x' = 0$, multiplied by the mass of tracer per unit area of fracture of streamtube section normal to flow, M. Flowrates in the tracer injection borehole were large enough such that reverse flux behind the origin, $x < 0$, could not take place. Therefore, presuming that the tracer and fluid are perfectly mixed at the wellbore face, the appropriate boundary condition at $x = 0^+$ is third-type. The following initial and boundary conditions describe the tracer test conditions in a semi-infinite medium:

$$C(x,0) = 0 \tag{2}$$

and

$$-D_L \frac{\partial C}{\partial x}(0,t) + vC(0,t) = M \cdot \delta(x) \tag{3}$$

$$C(+\infty,t) = 0 \tag{4}$$

The solution of equation (1) subject to (2), (3) and (4) can be obtained using the Laplace transform method. Expressed in dimensional form, it is written as:

$$C(x,t) = \frac{M}{\sqrt{\pi D_L t}} \exp\left\{-\frac{(x-vt)^2}{4D_L t}\right\} - M\left\{\frac{v}{2D_L}\right\} \exp\left\{\frac{vx}{D_L}\right\} \cdot \operatorname{erfc}\left\{\frac{x+vt}{2\sqrt{D_L t}}\right\} \tag{5}$$

where erfc is the complimentary error function. For Peclet numbers ($P_e = L/\alpha_L$) of greater than 10, the more easily obtained solution for a doubly infinite medium will provide adequate approximation (Sauty, 1980). However, since Peclet numbers in the order of 10 or less are expected (Raven and Novakowski, 1984; Novakowski et al., 1985a), the solution as given in (5) will be used as the basis for all advection-dispersion (AD) modeling.

The concentration-time data, C(t), as obtained from the transport models and the field tests are expressed as residence time distribution curves, E(t), first popularized by Danckwerts (1953) for use in chemical reactors. The residence time distribution (RTD), is defined as: E(t)dt being the fraction of fluid exiting a flow-through system whch possesses a residence time within the system of between t and t+dt. The E(t) curve is determined from the concentration-time response, C(t), of a flow-through system to a pulse injection of tracer by:

$$E(t) = \frac{C(t)Q}{M_{inj}} \qquad (6)$$

where Q is the steady volumetric flow rate through the system and M_{inj} is the mass of injected tracer.

Advection-Dispersion with Transient Solute Storage (ADTS) Model

If immobile fluid zones capable of transient solute storage exist and solute exchange between the storage zones and the longitudinally flowing fluid obey a first-order type exchange relation, equation (1) can be given as (Coats and Smith, 1964):

$$\phi \frac{\partial C}{\partial t} + (1 - \phi) \frac{\partial C_s}{\partial t} = -v \frac{\partial C}{\partial x} + D_L \frac{\partial^2 C}{\partial x^2} \qquad (7)$$

where ϕ is the mobile or flowing fraction of the total fracture pore space and C_s is the concentration in the immobile fluid or solute storage zone. Solute exchange between the mobile and immobile zones is determined simply by the differences in concentration and an exchange coefficient. The governing equation for the storage zone is (Lapidus and Amundson, 1952):

$$(1 - \phi) \frac{\partial C_s}{\partial t} = K(C - C_s) \qquad (8)$$

where K is the mass transfer coefficient. Equation (8) is given assuming that solute within the storage zone is uniformly and instantaneously distributed. As suggested by Bencala and Walters (1983), equation (8) simply describes what is likely a more complex process.

The analytical solution to equations (7) and (8) for impulse injection of tracer in a semi-infinite system has been solved by

Villermaux and Van Swaaij (1969) for initial and boundary conditions similar to those given for equation (1):

$$C(x,0) = C_s(x,0) = 0 \tag{9}$$

$$C(\infty,t) = C_s(\infty,t) = 0 \tag{10}$$

and

$$-D_L \frac{\partial C}{\partial x}(0,t) + vC(0,t) = M \cdot \delta(x) \tag{11}$$

The solution of Villermaux and Van Swaaij was obtained using Laplace transform methods for dimensionless forms of equations (7) - (11). The solution expressed as E(t) is a function of four parameters, Peclet number, P_e, plug flow transit time, τ, flowing fluid fraction, ϕ, and a dimensionless mass exchange constant, N, where $N = Kt$ (Van Swaaij et al., 1969). For a complete derivation of the solution refer to Villermaux and Van Swaaij (1969).

The influence of N and ϕ on the E(t) curves as obtained from the Villermaux and Van Swaaij solution was investigated and is shown in Figures 1 and 2. Figure 1 shows the influence of N, for $P_e = 6$, $\tau = 22$ h and $\phi = 0.60$. For $N = 0$, or no solute exchange, the resultant E(t) is that for the simple advection-dispersion model. With large N (i.e. $N \geq 10$) or rapid exchange of solute relative to fluid velocity, the E(t) curves have a similar form, except that the curves are lagged in time with respect to the $N = 0$ curve by a factor

directly proportional to the immobile fluid fraction. Between these two extreme cases, the curves are characterized by varying assymetries and long tails. In the range N = 1-2 the curves are characterized by a rapid rise in concentration, a well defined and narrow peak and a very slowly decaying tail. Figure 2 shows the influence of ϕ for $P_e = 6$, $\tau = 22$ h and N = 1.5. For $\phi = 1.0$, the E(t) curve reduces to the simple advection-dispersion model. With decreasing ϕ, the peak concentration attenuates and the position of the peak shifts slightly. Long slowly decaying tails are evident in Figure 2 for $\phi = 0.40 - 0.70$.

Flow Field Geometry

The tracer experiments were conducted using radial-convergent flow or in an injection-withdrawal format between two boreholes. To apply the transport models, a determination of the velocity field in the fracture is required. This determination for both types of experiments is made based on the fracture aperture, i.e. 2b, and the measured hydraulic gradient as expressed in the cubic law (Schlitching, 1968).

For the injection-withdrawal tracer experiments, velocity is determined from the streamline and velocity potential equations (Muskat, 1937; Hoopes and Harleman, 1967; Grove and Beetem, 1971; Novakowski et al., 1985a) where the flow field is divided into a series of streamtubes and one-dimensional transport is solved along

each streamtube. The length of each streamtube, L, is given as (Grove and Beetem, 1971):

$$L = \frac{2a\theta}{\sin \theta} \tag{12}$$

where θ varies positively from 0 to π and a is the half-distance between the injection and withdrawal boreholes. The time required for a particle of water to travel from the injection to withdrawal borehole, t_o, is derived from the velocity potential and upon substitution of the cubic law is written as:

$$t_o = \frac{a^2\ 24\ \mu}{\Delta H\ (2b)^2\ \rho g} \ln \left(\frac{2a}{r_w}\right) \left(\frac{1 - \theta\cot\theta}{\sin^2 \theta}\right) \tag{13}$$

where dynamic viscosity, μ, mass density, ρ, and gravitational acceleration, g, describe the flow properties of the fluid, r_w is the radius of the injection borehole and ΔH is the net imposed hydraulic head measured between the two boreholes. The velocity along each streamtube is obtained directly from equations (12) and (13) assuming that the injection and withdrawal flowrates are maintained equal, the natural gradient is small compared to the induced gradient and flow obeys the cubic law for a smooth parallel-plate model.

The velocity field for the radial convergent case is determined in a similar manner to the above except that the streamline length is given by the radial distance, r_o, from the pumping borehole axis to the borehole where tracer was injected and the travel time for plug flow, t'_o is determined from (Novakowski et al., 1985b):

$$t'_o = \frac{\ln (r_o/r_w)}{2} \cdot \frac{12\,\mu}{\rho g\,(2b)^2} \frac{(r_o^2 - r_w^2)}{\Delta H} \qquad (14)$$

Again this expression assumes that the natural gradient is negligible compared to the induced gradient and flow is according to the cubic law in a parallel-plate model.

SITE DESCRIPTION

Field tracer tests in a single fracture were performed at a study site located on the property of the Chalk River Nuclear Laboratories, Atomic Energy of Canada Ltd., approximately 200 km northwest of Ottawa, Ontario. The Chalk River area is part of the Grenville Structural Province of the Canadian Precambrian Shield. Regionally the bedrock is composed of metasediments and igneous suites which have been subject to polyphase deformation. Locally the study site is underlain by a folded sheet of quartz monzonitic gneiss with inclusions of metagabbro, pegmatite and diabase. Average fracture spacings of 1.0 m have been measured in surface outcrops and in boreholes at the study site. Additional descriptions of the geology and hydrogeology of the study site and of an adjacent test area are given by Raven and Novakowski (1984) and Novakowski et al. (1985a) respectively.

The tracer tests described in this paper were performed as part of a study investigating groundwater flow and solute transport in fractured low-permeability rock. The investigations were conducted in a series of 17 boreholes drilled using air percussion and diamond drill techniques to an average depth of 50 m in a 150-m by 200-m area (Figure 3). Each of the boreholes were geologically and geophysically logged, hydrogeologically tested and completed with multiple-packer monitoring casing to identify and characterize large fractures for subsequent hydraulic interference testing and tracer testing. Several large fractures were identified from the logging, hydraulic testing and monitoring.

In this paper, the hydraulic and dispersive properties of one large fracture intersected by six boreholes at depths of 20-35 m at the southern end of the study site are described.

Hydrogeologic Characterization of the Fracture

The location, orientation and extent of the fracture was evaluated from fracture logs and the results of injection and hydraulic interference testing. The natural groundwater flow pattern in the fracture was determined from periodic measurements of the hydraulic-head distribution over about three years and the character of the groundwater was determined from the geochemistry of several groundwater samples obtained from the fracture.

Each borehole drilled at the study site was systematically profiled using an injection-test technique with a straddle-packer spacing between 1.5 m and 2.0 m in length. The measured steady-state flowrates, Q, and injection heads, ΔH_{inj}, were analysed using the cubic law to obtain the aperture of the fracture for each test. Based on these results and in conjunction with the compiled fracture logs, the fracture intersection in each borehole was preliminarily identified. Subsequently, hydraulic interference tests were conducted to evaluate the extent of the hydraulic communication between the supposed intersections. The interference tests were performed by pumping one borehole and monitoring the drawdown in other boreholes in which the fracture intersection had been isolated. These tests were analysed using type-curve methods that account for wellbore storage capacity in the observation test interval (Chu et al., 1980). Following the hydraulic interference tests, more injection tests were completed in boreholes FS-6, 11 and 15 using a shorter packer spacing (0.75 m) over the 1.5-2.0 m intervals that showed interconnection between boreholes. Table 1 lists the fracture apertures calculated from both the injection tests (entries under the same activation and observation borehole) and the hydraulic interference tests.

The injection test and hydraulic interference test results show that the fracture has a radial extent of about 50 m, a relatively uniform opening of about 110-190 μm in the central portion (in the vicinity of boreholes FS-6, 11 and 15) and reduced opening to the north, south and west. The fracture was located using the results of

the short-interval injection tests and the fracture logs, at depths of 34.6, 33.6 and 35.8 m along boreholes FS-6, 11 and 15 (Figure 4) and dips at about 25° to the northeast.

Hydraulic head measurements obtained from the fracture indicate natural groundwater flow to the northeast in the dip direction of the fracture with gradients of 0.001 - 0.1. The hydraulic gradients between boreholes FS-6, 11 and 15 are the smallest (0.001-0.002) reflecting the relatively uniform and large opening of the fracture in this area.

Chemistry of the groundwater in the fracture was determined from analysis of samples repeatedly collected over a 2-3 year period prior to tracer testing. The groundwater is Ca-HCO_3 type with pH 8.0, Eh 0.20 V, specific conductance 20 $mS \cdot m^{-1}$ and low ionic strength (0.005). Na, Mg-SO_4 are the second most dominant ion groups. Calculations performed using an equilibrium chemical speciation program (WATEQF, Plummer et al., 1976) indicate saturation of the groundwater with respect to calcite, quartz, and several Fe oxides and Ca-Mg silicates. Inspection of fracture surfaces in recovered core corroborates these calculations, with calcite and to a lesser extent chlorite being the dominant fracture infilling minerals observed.

Groundwater samples collected prior to tracer testing had background tracer concentrations of less than 2 $\mu g \cdot L^{-1}$ Na Fluorescein and about 0.1 - 0.2 $KBq.L^{-1}$ activity for ^{82}Br.

FIELD TRACER TESTS

Methodology

Five tracer tests were performed in the three-borehole array of boreholes FS-6, 11 and 15. The tracer experiments were performed in the central high-permeability region of the fracture to reduce far-field boundary effects or distortion of the flow field. The test conditions of each of the tracer experiments are summarized in Table 2. During tracer test no. 1, radioactive gamma-emitting ^{82}Br was injected in an injection-withdrawal flow field established without recirculation and pumped at equal rates between borehole FS-6 (injection) and borehole FS-15 (withdrawal). In the second tracer experiment, Na Fluorescein was injected in a similar flow field, except that the injection borehole (FS-15) and the withdrawal borehole (FS-6) were reversed from the first test. Radioactive ^{82}Br was used as the tracer in the third test, which was performed in a radial-convergent flow field towards borehole FS-15 from borehole FS-6. Tracer tests no. 4 and no. 5 were conducted together between boreholes FS-6, 11 and 15 using radiaoctive ^{82}Br as tracer. During these tests an injection-withdrawal flow field with recirculation of withdrawn fluid was established between boreholes FS-6 (injection) and FS-11 (withdrawal) and breakthrough of tracer was monitored at both the withdrawal borehole (test no. 5) and the passive intervening borehole, FS-15 (test no. 4).

Straddle-packer assemblies of short interval length were used to isolate the communicating fracture and to reduce the test interval volume and the mean residence time of tracer in each borehole. Test interval lengths of 0.88, 0.74 and 0.64 m corresponding to test interval volumes of 6.0, 5.1 and 2.0 L were determined from dimensions of the packer assemblies and of the boreholes for the test intervals in boreholes FS-6, 11 and 15 respectively. The small test interval volumes were achieved in part by constructing the borehole probes with plastic pipe of a diameter slightly less than the diameter of the borehole.

Steady flow conditions were established in the fracture approximately 5-10 h prior to tracer injection for each tracer test. Steady flow conditions were assumed with the attainment of steady hydraulic heads (±0.05 m) and flow rates (±3%). Hydraulic heads and flow rates were continuously monitored at each borehole throughout each test using submersible pressure transducers and turbine flow meters. Table 2 summarizes the steady hydraulic head and flow rate conditions measured during each tracer test. The hydraulic heads listed in Table 2 are the sum of the net changes in hydraulic head from equilibrium values for both the injection and withdrawal boreholes. The data in Table 2 shows that the imposed hydraulic gradients are greater than 25 times the natural field gradients.

Prior to tracer tests no. 1 and no. 2, groundwater for subsequent injection was pumped from the fracture and stored under nitrogen gas in a 2000-L epoxy-lined fluid reservoir. Monitoring of pH and Eh

during pumping and reinjection indicated a negligible change in chemistry of the groundwater during this temporary surface storage.

Radioactive ^{82}Br tracer was injected as a 2 mL solution of KBr using a hypodermic needle inserted through a septum installed in the injection tubing at surface. The Na Fluorescein tracer was pumped into the injection tubing at surface as a 100 mL solution at a concentration of 1000 $mg.L^{-1}$. The surface injections of all tracers were virtually instantaneous, being completed in less than 15 s. The mass of tracer injected in each test is shown in Table 2 and was determined from concentration analyses of aliquots of the injected tracer solution.

The residence time distributions of radioactive tracer in the injection interval were measured using a gamma detector probe positioned in the centre of the plastic pipe of the packer assembly at the depth of the intersection fracture. The downhole probe was coupled to a scaler rate meter.

During tracer test no. 3 (the radial convergent flow field test) the radioactive tracer was flushed into the injection test interval and out into the fracture by injecting groundwater at a rate of 1.0 $L.min^{-1}$. Groundwater was pumped until the tracer concentration in the injection interval reduced to 20% of the peak concentration or 13 min after tracer injection at surface.

Breakthrough of tracer at the withdrawal boreholes was determined by sampling the withdrawn groundwater and analysing the samples for tracer concentrations in the laboratory using liquid scintillation

counting equipment for the radioactive tracer and a fluorometer for the fluorescent dye tracer. During tracer tests no. 4 and no. 5 all of the withdrawn groundwater except for the negligible amount collected for samples was reinjected into boreholes FS-15 and FS-6 respectively. Groundwater was withdrawn and reinjected in borehole FS-15 so as not to perturb the flow field established between boreholes FS-6 and FS-11. Groundwater withdrawn from borehole FS-11 was reinjected in borehole FS-6 because of the lack of a sufficiently large storage reservoir for the injection fluid. Tracer breakthrough at the withdrawal boreholes was also monitored at surface using a gamma detector and a field fluorometer installed as flow-through cells on the discharge line of the withdrawal boreholes.

Breakthrough of radioactive tracer in the withdrawal test intervals was monitored using a second gamma detector probe located within the plastic pipe of the withdrawal packer assembly and positioned opposite the fracture in a manner similar to that used in the injection interval. The residence time distributions of tracer in the injection interval, in the withdrawal interval and at surface were measured to determine the effect of mixing in both the injection and withdrawal borehole instrumentation on the RTD curves for the fracture.

Results

The residence time distributions of radioactive tracer in the injection interval of borehole FS-6 for tracer tests no. 1, 3, 4 and 5

are shown in Figure 5. The curves are plotted as relative count rate C/C_p where C_p is the peak count rate and counts are corrected for radioactive decay. Actual tracer concentrations were not determined because of an unknown counting efficiency for the particular counting geometry. The curves are slightly skewed with a rapid initial rise in count rate and slow decay after the peak. Although no information on the distribution of tracer residence time in the injection interval in borehole FS-15 is available for tracer test no. 2, we can assume in the worst case a similar distribution to those shown in Figure 5 because of the similar injection flow rates and the smaller volume of the injection test interval in borehole FS-15.

Residence time distribution curves for tracer in the fracture were determined primarily from tracer concentration analyses of groundwater samples collected at the withdrawal borehole. The resulting RTD curves corrected for plug flow transit time in the injection and withdrawal tubing and corrected for radioactive decay are shown in Figures 6 to 10. Table 3 summarizes some of the characteristics of the fracture RTD curves such as time to peak concentration, t_p, peak concentration, C_p, peak of the RTD, E_p, relative concentration C/C_p at the end of the test, and truncated mass recoveries, m_{rec}.

The RTD curves determined from the gamma counters positioned in the withdrawal boreholes were identical in shape to the RTD curves determined from groundwater samples for tracer tests No. 1, 3 and 5 and are shown for tests no. 1 and no. 3 in Figures 6 and 8. The gamma

counter response for tests no. 1 and no. 3 are plotted in Figures 6 and 8 as E(t) by determining a counting efficiency for the gamma probe in FS-15 from comparison of tracer concentrations in groundwater samples and the signal from the downhole gamma probe.

The counting efficiency measured during tracer test no. 3 was used to determine effective tracer concentrations of the interval fluids in borehole FS-15 during passive monitoring of breakthrough as part of tracer test no. 4. As shown in Figure 9 the RTD curve determined from the downhole counter is different from the RTD curve determined from groundwater samples. The lower peak concentration and time lag of the RTD curve determined from groundwater samples collected at surface suggests incomplete mixing of groundwater between the fracture and test interval and in the test interval. This incomplete mixing is possible as the injection and withdrawal ports used for recirculating the interval fluids to surface were located at approximately the same elevation in the test interval. The response from the downhole gamma counter represents the RTD curve for an unknown number of streamtubes that are sampled by borehole FS-15. Because of this passive monitoring of tracer breakthrough in streamtubes and the proximity of FS-15 to the injection borehole, the flow field of test no. 4 for modelling purposes is assumed to be radial and the mass transport, one-dimensional.

Because tracer test no. 5 was performed with recirculation of the withdrawn fluid, the tracer breakthrough at intermediate-to-late time is a result of both the initial pulse injection of tracer and tracer reinjected with the recirculated groundwater. Analysis of the tracer

experiment is simplified by assuming that the tracer breakthrough curve results only from the initial pulse injection of tracer. By assuming an initial pulse or Dirac impulse injection of tracer, the RTD curve without recirculation effects, E(t), can be determined from the RTD curve with recirculation effects, $E_r(t)$ calculated from the measured concentration-time data by applying the convolution integral as given by Levenspiel (1972):

$$E(t) = E_r(t) - \int_o^t E_r\,(t - t')\,E(t')\,dt' \qquad (15)$$

The true RTD curve is therefore evaluated at each time t using measured concentration-time data at earlier times. The integral in (14) must be evaluated for each time point and was numerically determined using the trapezoidal rule between points. The true RTD curve and the RTD curve with recirculation effects for the tracer breakthrough measured during tracer test no. 5 are shown in Figure 10. Removal of the recirculation effect results in a true RTD curve with earlier and lower peak concentration.

Fractional mass recovery, m_{rec} for each tracer test is evaluated by integrating the complete RTD curve:

$$m_{rec} = \int_o^\infty E(t)dt \qquad (16)$$

Because the field curves are typically characterized by long tails at low concentrations and the tracer tests were terminated at relative tracer concentrations, C/C_p, on the tail of 0.25 - 0.50,

only truncated mass recoveries can be reliably reported. The truncated mass recoveries calculated for the observed RTD curves are listed in Table 3 and range between 0.45 and 0.65. These high mass recoveries and the approximate exponential decay of the RTD curves, suggest that it is reasonable to assume complete mass recovery would be obtained with extrapolation of the RTD curves to much later time. It is important to note that the fractional mass recovery of tracer test no. 4 reflects the recovery mass in an unknown number of streamtubes passively sampled by borehole FS-15 and not the mass recovery for the entire fracture.

INTERPRETATION AND DISCUSSION

Modelling the Field Data

Simulations of the AD model and of the ADTS model were visually fit to the field data to determine model parameters. The fitting procedure was complicated by the fact that both simulation models express the mass of injected tracer as a fictitious concentration uniformly distributed over the total fluid volume, V_f, of the fracture between the injection and withdrawal boreholes, and that this volume is usually not well defined, particularly in rough, heterogeneous fractures. Therefore M, the injected tracer mass per unit section of fracture or streamtube normal to flow in boundary conditions (3) and (11) must be determined from:

$$M = \frac{M_{inj} L}{V_f} \tag{17}$$

Because of uncertainty in V_f, the fitting between the model simulations and the field data was performed with both RTD curves expressed in relative form E/E_p. This is equivalent to fitting to the shape and the position of the field data curve and has previously been used by Sauty (1980) for advection-dispersion parameter estimation from tracer tests performed in porous media and by Novakowski et al. (1985a) for tests in a single fracture. Tracer tests no. 1, 2 and 5 were fit with the AD and ADTS models considering the geometry of the injection-withdrawal flow field. Tracer tests no. 3 and no. 4 were fit with the models assuming that the flow fields could be approximated as radial. For Peclet numbers of greater than 1-3 uniform, one-dimensional solute transport can be approximated by radial solute transport (Sauty, 1980) and therefore will suffice in modeling tracer tests no. 3 and no. 4 (Peclet numbers of 6 and 14, respectively).

It was not possible to fit the AD model to the complete RTD curve determined from the field data for four of the five tests. Only the rising portion and the position of the peak of the field RTD curve were fit to obtain AD model parameters of α_L and 2b respectively. The post-peak portion of the field RTD was not fit because of the assumed effects of transient solute storage. The model parameters of parallel-plate opening and longitudinal dispersivity are both estimated to be accurate to ±5%, meaning that changes in model

parameters greater than this amount resulted in noticeably poorer quality fits.

The ADTS model was fit to the field RTD curve by using the AD model parameters of 2b and α_L. This was done because 1) all the field RTD curves were characterized by similar highly assymmetric shapes which are representative of a particular range of N (1.0 - 2.0) and ϕ (0.40 - 0.70) model parameters and 2) for these ranges of N and ϕ model parameters, the initial breakthrough, the rising portion and the position of the peak of the RTD curves from the ADTS model are not substantially different than the AD model simulations (equivalent to the ADTS model with N = 0 and ϕ = 1.0 in Figures 1 and 2), particularly when the RTD curves are expressed in relative form. The greatest difference occurs in the position of peak of the RTD curve which changes at most by 15-20%.

Using the AD model parameters of 2b and α_L, it was possible to fit to virtually the entire field RTD curve expressed in relative form by varying ϕ and N model parameters. The ADTS model-fitted parameters are listed in Table 4 and are estimated to be accurate to ±10%.

The best fit AD and ADTS model RTD curves in relative form were plotted against the field data as E(t) in Figures 6 to 10 by determining the total volume of the fracture, V_f, between the injection and withdrawal boreholes in each test. The total volume of the fracture or of an individual streamtube in the fracture was determined from:

$$V_f = \frac{\zeta Q t}{\phi} \qquad (18)$$

where $Q\tau/\phi$ is the theoretical fracture or streamtube volume (Danckwerts, 1953) derived by the model and ζ is an empirical coefficient determined from the ratio of the RTD values of the field data and the best fit of the model. The ζ coefficient expresses the deviations of the theoretical fracture volume from the observed fracture volume required to fit the model to the field data, as a result of roughness effects and other nonideal flow conditions. The ζ values (Table 4) were determined from the best fits of the ADTS model because of the quality of the fits over the entire field RTD curves. The ζ values range from 0.68 to 1.24. Values of ζ less than one mean that the actual fracture volume is less than the theoretical value, while ζ values greater than one indicate that the actual fracture volume is greater than the theoretical value.

Interestingly, the ζ values for the tracer tests conducted between FS-6 and 15 are all similar and greater than 1.0, whereas the ζ value for test no. 5 which was conducted in the southern part of the fracture is less than 1.0. This suggests that the actual fracture volume is largest in the central portion of the fracture probably due to the predominance of large irregular void space. The result for test no. 5 is probably due to the influence of the reduced aperture in this portion of the fracture.

Influence of Borehole Instrumentation on Fracture RTD Curves

RTD curves from tracer tests performed in fractured low-permeability media can often be influenced by long residence times of

tracer in the borehole and in the borehole instrumentation as a result of the low rates of flux through the media and the large mixing volumes in the borehole and borehole equipment (Novakowski et al., 1985a). In the tracer tests reported here, the residence time of tracer in the boreholes and in the borehole instrumentation was minimized and for the radioactive tests, measured using downhole gamma detectors.

The influence of the withdrawal borehole and test equipment on the RTDs can be qualitatively evaluated by comparing the RTDs measured by the downhole gamma detector with those determined from analysis of groundwater samples collected at surface. The identical shapes of the two RTDs observed during tests no. 1, 3 and 5 indicate a negligible effect. Because of similar flow rates, test interval volumes and RTDs we can assume a similar negligible effect of withdrawal borehole and test equipment on the RTD curve for tracer test no. 2. Test no. 4, however, shows a significant effect of withdrawal borehole and test equipment, likely a result of poor mixing within the withdrawal interval.

The influence of the injection borehole and test equipment on the RTDs measured at the withdrawal boreholes can be quantitatively evaluated by comparing the means and time-dependent variances of the RTDs measured in the injection intervals and at the withdrawal boreholes. In fact, by using the additive properties of the means and variances developed for closed and independent vessels in series (Levenspiel, 1972), the means and variances of the fracture RTDs can

be determined from simple subtraction of these values determined at each borehole. Using the method of moments, the means and variances of the RTD curves measured at the withdrawal boreholes and depicted in Figures 6-10 can be shown to be in the ranges 9.0 - 83.0 h and 72 - 6700 h^2, respectively. The means and variances of the RTDs measured in the injection boreholes average 0.12 h and 0.008 h^2, respectively, which is negligible in comparison to the values calculated from the RTDs measured at the withdrawal boreholes. From these comparisons it can be assumed that the RTDs measured at the withdrawal borehole and shown in Figures 6-10 are the RTDs of the fracture.

AD and ADTS Model Results

The parallel plate openings, 2b, determined from the tracer tests performed between boreholes FS-6 and FS-15 (test nos. 1-4) are similar (90 - 115 μm) for different test conditions but different than the opening determined from tracer test no. 5 (45 μm) indicating a reduction of opening and fluid velocity in the fracture between boreholes FS-15 and FS-11.

The variation of model parameters α_L, $\bar{K}$ ($\bar{K} = N/\bar{\tau}$, where $\bar{\tau}$ is mean plug flow transit time of a tracer test) and ϕ observed from fitting to test nos. 1 - 4 for relatively uniform 2b, suggests velocity or residence time effects in determination of these parameters. To identify these effects the model parameters of $\bar{K}$ and α_L were plotted against mean fluid velocity $\bar{v}$, in Figures 11 and

12. Mean fluid velocity and mean plug flow transit time for the injection-withdrawal tests were calculated from the averages of these values for individual streamtubes which theoretically contribute to the model RTD to the end of field test. Also, since tracer test no. 5 was performed over two parts of the fracture (i.e. FS-6 to FS-15 and FS-15 to FS-11) which have different opening and fluid velocity, it was necessary to determine value of $\bar{v}$, $\bar{K}$ and α_L for the fracture between boreholes FS-15 and FS-11. These parameters were calculated from the AD model parameters of tracer test no. 5 and tracer test no. 4 using the additive properties of means, $\bar{t}$ and variances, σ^2, of RTDs assuming that the mean residence time, $\bar{t}$ is approximated by the mean plug flow transit time, $\bar{\tau}$. The longitudinal dispersivity α_L was determined from the variance using the exact relation given by Levenspiel (1972), for flow-through systems subject to a Dirac impulse injection of tracer:

$$\sigma^2_{out} - \sigma^2_{in} = \frac{2\bar{t}^2\alpha_L}{L} \qquad (19)$$

where σ^2_{in} and σ^2_{out} are the time-dependent variances of the RTDs into and out of a fracture which results from advection-dispersion processes. An α_L of 5.0 m was determined for the fracture between boreholes FS-15 and FS-11.

Figure 11 shows a roughly linear increase in the mean mass transfer coefficient, $\bar{K}$, with mean fluid velocity indicating faster mixing between the flowing and immobile fluid with increasing

velocity. Coats and Smith (1964) and Van Genuchten and Wierenga (1977) observed similar effects in laboratory experiments. The increase of $\bar{K}$ with $\bar{v}$ is likely explained by convective rather than diffusive exchange between flowing and immobile fluid zones. Such convective mixing may result from the transfer of mass into cavities and stagnant zones by flow vortices created at sharp turns along the fracture wall and around asperities (see Van Dyke, 1982 for visualized examples). Subsequent mass return would occur continually by entrainment of the material from vortices and eddies into the main stream. These processes can take place in flow at Reynolds number, Re, much less than one but are exemplified as velocity increases (Re increases). The Re calculated for the tracer experiments range from 1-50 where highest Re are near the pumping or injection boreholes and depend on the volumetric flowrate.

Table 4 in conjunction with the mean fluid velocities determined for the tracer tests and shown in Figure 11, indicate an approximate increase in the immobile fluid fraction $(1-\phi)$ with increasing fluid velocity. This result is opposite to the observations of Coats and Smith (1964), Villermaux and Van Swaaij (1969) and Van Genuchten and Wierenga (1977) for laboratory experiments with porous media, opposite to qualitative observations made by Maini (1971) in dye experiments on plastic molds of natural fractures and opposite to observations made in river-mixing studies (Pederson, 1977; Bencala and Walters, 1983). The immobile fluid fraction-velocity relation indicated by the tracer experiments could be due to the increase in the volume of stagnant

zones around asperities and flow constrictions as a result of laminar flow separation and wake effects and enlargement of the boundary layers created by increasing flow velocity. Thus with increasing fluid velocity more of the tracer may be carried by an "inertial core" (Dybbs and Edwards, 1984) of fluid flowing outside the boundary layers on the fracture walls, while at lower velocities the tracer would be distributed more uniformly between the "inertial core" and the slower velocity fluid. Such "inertial cores" have been observed by Dybbs and Edwards (1984) in streakline studies of flow through plexiglass models of porous media at Re as low as 1-10.

Figure 12 shows an increase in longitudinal dispersivity, α_L, with decreasing fluid velocity below 2 $m.h^{-1}$ and relatively uniform α_L above 2 $m.h^{-1}$. This variation of α_L with velocity is important because it shows that induced gradient tracer tests are likely to underestimate the dispersive characteristics of fractures under natural flow conditions. The observed dispersivity-velocity relation may also be explained by the dominance of advection in the transport process and the development of "inertial cores" of flowing fluid. At lower fluid velocity the tracer may be more uniformly distributed between the fluid of the higher velocity "inertial core" and the lower velocity boundary layers resulting in larger values of α_L. At higher fluid velocity the α_L is likely determined from the distribution of fluid velocities within the "intertial core" which appear to be similar over the range of $\bar{v}$ of 2-5 $m.h^{-1}$.

The concept of an initial advective-dominated period progressing to Fickian-type behaviour as observed in analogous studies can also be qualitatively evaluated for studies of solute transport in single fractures by comparing the goodness of fit of the AD models to the field data for increasing tracer residence time. The tracer tests arranged in order of increasing mean residence time (i.e. nos. 2, 1, 4, 3 and 5) show improved fit of the AD models to the field RTDs (Figures 7, 6, 9, 8 and 10). In fact, the slowest velocity-longest distance test (test no. 5) can be fit with the AD model over the entire RTD. This trend suggests that solute transport within the fracture under natural flow conditions with much longer tracer residence times may be described by a simple advection-dispersion model. Furthermore, these experimental results and trends confirm for single fractures, the supposition of Coats and Smith (1964) that the transient solute storage effect may have little importance in causing assymmetry or mixing under natural-gradient field conditions, but nevertheless may be very important in interpreting field and laboratory tracer experiments of much shorter duration.

Comparison of Fracture Opening Determined from Hydraulic Tests and Tracer Tests

Comparison of openings, 2b, determined from hydraulic tests and from tracer tests provides an assessment of the validity of the smooth, parallel-plate model or cubic law in describing both the fluid flow rate and fluid velocity properties of fractures. This assessment

is valuable because often it is impractical to complete tracer experiments and average fluid velocities must be inferred from hydraulic tests using a simple model, which in the case of single fractures, is invariably the smooth, parallel-plate model.

The fracture openings determined from hydraulic tests performed in and between the tracer test boreholes show an average opening of 135 μm and range from 110-190 μm. These openings are larger than the average 2b estimates determined from the tracer tests at about 100 μm (FS-6 to FS-15) and 45 μm (FS-6 to FS-11) suggesting that actual fluid velocities were 2-10 times slower than predicted using the results of hydraulic tests interpreted using the smooth parallel-plate model. Similar observations from hydraulic and tracer tests performed in single fractures have been reported by Abelin et al. (1983) and Novakowski et al. (1985a), although the opposite result, that of faster tracer velocities has also been measured (Raven and Novakowski, 1984). The differences in opening and velocity suggest that the cubic law may not be appropriate in describing both the fluid flow rate and velocity properties of natural fractures.

The slower velocities observed from tracer experiments are thought to be generally characteristic of the fluid flow properties of rough fractures as a result of 1) tortuous flow pathways created by roughness, 2) fluid entrapment and advective exchange in secondary flow vortices and immobile fluid zones within the fracture and 3) inertial head losses caused by sharp turns in the flow path and the continual acceleration and deceleration of fluid as it is forced in constricted regions and expands into subsequent enlargements of the fracture plane.

Influence of Rock Matrix Diffusion on Fracture RTDs

Diffusion of solute from a fracture into a porous rock matrix has been recognized as an important transport process in fractured low-permeability rock (Grisak and Pickens, 1980). Such a process might explain the skewness of the fracture RTDs presented in this paper. However, matrix diffusion effects are, based on the theoretical work by Maloszewski and Zuber (1985) and available measures of intact rock porosity, η, and diffusion coefficient, D_p, only of minor importance in these short-duration experiments and cannot explain the observed skewness of the RTDs. Maloszewski and Zuber show that for tracer experiments of tens of hours duration, matrix diffusion has a negligible effect on a fracture RTD when the ratio of matrix to fracture porosity expressed as their a parameter ($a = \eta\sqrt{D_p}/2b$) is small (i.e. $\leq 10^{-4}$). Using reasonable values of η (3×10^{-3}) and D_p (10^{-10} m^2 s^{-1}) for intact granite (Bradbury and Green, 1985; Skagius and Neretnieks, 1986) and 2b determined from hydraulic tests (135 μm), the likely a parameter of the fracture-matrix system tested is small at 2×10^{-4}. This low a parameter indicates a negligible effect of matrix diffusion on the field RTDs.

In addition, the interpretation that solute exchange between the flowing and immobile fluids results from convective rather than diffusive processes indirectly suggests that matrix diffusion is not a significant transport process in the tracer tests.

CONCLUSIONS

Five induced-gradient tracer tests were performed in a single fracture under five different fluid velocities. The tracer breakthrough curves were interpreted using residence time distribution (RTD) theory developed for use in chemical reactors and two deterministic simulation models adapted for use in single fractures. The simulation models were a simple two parameter, advection-dispersion (AD) model and a four parameter advection-dispersion with transient solute storage (ADTS) model. Model parameters were determined for each tracer test by fitting the model simulations to the field RTDs.

The quality of fits observed between the two simulation models and the field RTDs indicate the existence of an initial advective-dominated period of solute transport progressing to Fickian-type behaviour with increasing tracer residence time or decreasing fluid velocity. Similar observations have been made in analogous studies of dispersion in conduits, rivers and stratified aquifers. Because the tracer experiments were induced-gradient tests, this observation further indicates that dispersion of a conservative solute within single fractures under natural flow conditions may be described by a simple advection-dispersion model, provided, of course, that nonhydrodynamic transport processes such as matrix diffusion are appropriately considered.

The advection-dispersion with transient solute storage model provided excellent fits to the field RTDs. While the quality of the fits does not prove that transient solute storage in immobile fluid zones actually occurs, the fits do show that such a model can account for the skewness frequently observed with single fracture tracer tracer tests of relatively short duration (<100 h) where matrix diffusion effects are likely of minor importance. This observation is important because application of the ADTS model to the tracer tests reported herein results in lower longitudinal dispersivities and higher mean fluid velocities than would be determined from the more traditional method of moment calculations. Variations of the model-derived mean mass transfer coefficient with mean fluid velocity further suggest that, if such processes exist, the solute exchange between the flowing and immobile fluid zones is likely convective rather than diffusive in nature.

Comparison and analysis of the RTDs measured in the injection and withdrawal test intervals and determined at surface from tracer analyses of groundwater samples quantified the effect of flow through the borehole instrumentation on RTDs of the fracture. The results generally show a negligible effect of borehole instrumentation on the fracture RTDs provided that the tracer residence times within the borehole test intervals and instrumentation are minimized and that rapid mixing is ensured within the borehole test intervals. These conditions can be easily achieved through careful tracer test design.

Comparison of fracture openings determined from the tracer experiments and from the hydraulic tests show that the cubic law or the smooth, parallel-plate model is not appropriate in describing both the fluid velocity and flow rate properties of natural fractures. The actual fluid velocities observed with the tracer tests were 2-10 times slower than the velocities predicted using the results of hydraulic tests interpreted using the cubic law.

The results of both model simulations of the field RTDs show a mean fluid velocity or residence time effect in the determination of longitudinal dispersivity, α_L in single fractures. The observed variation of α_L shows that induced gradient tracer tests are likely to underestimate the dispersive characteristics of fractures under natural flow conditions. While natural gradient tracer tests might theoretically reduce these effects and yield more representative dispersion parameters for predictive models, the heterogeneous hydraulic properties of fractures mitigate against the success and reliable interpretation of such tests. Given these constraints, there is a need to perform tracer experiments in natural fractures under induced gradients that approach natural flow conditions.

ACKNOWLEDGEMENTS

This work was supported by funds provided by the Whiteshell Nuclear Research Establishment and the Chalk River Nuclear Laboratories, both of Atomic Energy of Canada Ltd. as part of the Canadian Nuclear Fuel Waste Management Program. The authors

gratefully acknowledge the assistance of E.L. Cooper, D.R. Champ and J. Young, AECL in preparing and handling the radioactive tracers; B. Kueper, AECL; J. Scröter, University of Kiel, West Germany; and K. Inch, NHRI in performing the field experiments; and E. Hodgins, AECL in computer modeling. A special thanks is extended to D.R. Champ for co-ordination of the tracer testing program at the Chalk River Nuclear Laboratories.

NOTATION

a half distance between injection-withdrawal boreholes, m

a ratio of matrix to fracture porosity, $s^{-1/2}$

b half opening of an equivalent smooth, parallel-plate fracture, μm

C concentration of tracer in flowing fluid, $KBq.L^{-1}$ or $\mu g.L^{-1}$

C_p peak concentration of tracer in effluent, $KBq.L^{-1}$

C_s concentration of tracer in stagnant fluid or transient solute storage zones, $KBq.L^{-1}$

D_L coefficient of longitudinal hydrodynamic dispersion, $m^2.s^{-1}$

E residence time distribution function for a pulse injection of tracer, h^{-1}

E_p peak value of residence time distribution function, h^{-1}

E_r residence time distribution with recirculation effects, h^{-1}

g gravitational constant, equal to 9.81 $m.s^{-2}$

ΔH imposed hydraulic head, m

ΔH_{inj} injection head, m

K mass transfer coefficient, h^{-1}

$\bar{K}$ mean mass transfer coefficient of a tracer test, h^{-1}

L flow path or streamtube length, m

M mass of tracer injected per unit area of fracture or streamtube section normal to flow, $MBq.m^{-2}$ or $mg.m^{-2}$

M_{inj} mass of tracer injected as a pulse, MBq

m_{rec} fractional mass recovery

N mass exchange constant, dimensionless, equal to Kt

P_e Peclet number, dimensionless, equal to L/α_L

Q volumetric flow rate, $m^3.s^{-1}$

r_o radial ditance from pumping borehole to tracer injection borehole, m

r_w radius of borehole, m

t time, s or h

$\bar{t}$ mean residence time of tracer, h

t_p time of peak effluent concentration of tracer, h

t_o plug flow travel time, injection-withdrawal flow field, s or h

t'_o plug flow travel time, radial flow field, s or h

V_f fluid volume of a fracture between injection and withdrawal boreholes, m^3

v average linear groundwater velocity, $m.s^{-1}$

$\bar{v}$ mean groundwater velocity of a tracer test, $m.s^{-1}$

α_L longitudinal dispersivity, m

δ Dirac function

ζ empirical fitting coefficient, dimensionless

θ angle of arc length

μ dynamic viscosity of water, $Pa.s^{-1}$

ρ mass density of water, $Kg.m^{-3}$

σ^2 variance of RTD curve, h^2

σ^2_{in} variance of RTD entering a fracture, h^2

σ^2_{out} variance of RTD exiting a fracture, h^2

τ plug flow travel time of fluid in a streamtube or fracture, h

$\bar{\tau}$ mean plug flow transit time of a tracer test, h

ϕ flowing fluid fraction of fracture pore space, dimensionless

REFERENCES

Abelin, H., J. Gidlund and I. Neretnieks, Migration experiments in single fracture in the Stripa granite: Preliminary results, in Proc. of the Workshop on Geological Disposal of Radioactive Wastes, In Situ Experiments in Granite, Stockholm, Sweden, 154-163, Organization for Economic Co-Operation and Development, Paris, 1983.

Aris, R., On the dispersion of a solute in a fluid flowing in a tube, Proc. R. Soc. London Ser. A, 235, 67-77, 1956.

Aris, R., The longitudinal diffusion coefficient in flow through a tube with stagnant pockets, Chem. Eng. Sci., 10, 194-198, 1959.

Bencala, K.E. and R.A. Walters, Simulation of solute transport in a mountain pool-and-riffle stream: A transient storage model, Water Resour. Res., 19(3), 718-724, 1983.

Black, J.H. and K.L. Kipp, Jr., Movement of tracers through dual-porosity media - Experiments and modelling in the Cretaceous Chalk, England, J. Hydrol., 62, 287-312, 1983.

Bradbury, M.H. and A. Green, Measurement of important parameters determining aqueous phase diffusion rates through crystalline rock matrices, J. Hydrol. 82, 39-55, 1985.

Chatwin, P.C., The approach to normality of the concentration distribution of a solute in a solvent flowing along a straight pipe, J. Fluid Mech., 51(2), 321-352, 1970.

Chatwin, P.C., Presentation of longitudinal dispersion data, J. Hydraul. Div. Am. Soc. Civ. Eng., 106(HY1), 71-82, 1980.

Chu, W.J., J. Garcia-Rivera and R. Raghavan, Analysis of interference test data influenced by wellbore storage and skin at the flowing well, J. Pet. Tech., January, 171-178, 1980.

Coats, K.H. and B.D. Smith, Dead end pore volume and dispersion in porous media, Soc. Pet. Eng. J., 4, 73-84, 1964.

Danckwerts, P.V., Continuous flow systems: Distribution of residence times, Chem. Eng. Sci. 2, 1-13, 1953.

Dybbs, A. and R.V. Edwards, A new look at porous media fluid mechanics - darcy to turbulent, in Fundamentals of Transport Phenomena in Porous Media, Proc. NATO Advanced Study Institute on Mechanics of Fluids in Porous Media, Newark, Delaware, U.S.A., July 18-27, 1982, 201-256, 1984.

Elder, J.W., The dispersion of marked fluid in turbulent shear flow, J. Fluid Mech., 5(4), 544-560, 1959.

Elhadi, N., A. Harrington, I. Hill, Y.L. Lau and B.G. Krishnappan, River mixing - A state-of-the-art report, Can. J. Civ. Eng., 11, 585-609, 1984.

Fischer, H.B., Dispersion prediction in natural streams, J. Sanit. Eng. Div. Am. Soc. Civ. Eng., 94(SA5), 927-944, 1968.

Fischer, H.B., The mechanics of dispersion in natural streams, J. Hydraul. Div. Am. Soc. Civ. Eng., (93(HY6), 187-216, 1967.

Fried, J.J., Groundwater Pollution, 330 pp., Elsevier, New York, 1975.

Güven, O., F.J. Molz and J.G. Melville, An analysis of dispersion in a stratified aquifer, Water Resour. Res., 20(10), 1337-1354, 1984.

Gaudet, J.P., H. Jégat, G. Vachaud and P.J. Wierenga, Solute transfer, with exchange between mobile and stagnant water, through unsaturated sand, Soil Sci. Soc. Am. J., 41, 665-671, 1977.

Gelhar, L.W., A.L. Gutjahr and R.L. Naff, Stochastic analysis of macrodispersion in a stratified aquifer, Water Resour. Res., 15(6), 1387-1397, 1979.

Gill, W.N. and R. Sankarasubramanian, Exact analysis of unsteady convective diffusion, Proc. R. Soc. London Ser. A, 316, 341-350, 1970.

Grisak, G.E. and J.F. Pickens, Solute transport through fractured media, 1, The effect of matrix diffusion, Water Resour. Res., 16(4), 719-730, 1980.

Grove, D.B. and W.A. Beetem, Porosity and dispersion constant calculations for a fractured carbonate reservoir using the two well tracer method, Water Resour. Res., 7(1), 128-134, 1971.

Hays, J.R., Mass transport mechanisms in open channel flow, Ph.D. dissertation, Vanderbilt University of Nashville, Tennessee, 1966.

Hodgkinson, D.P. and D.A. Lever, Interpretation of a field experiment on the transport of sorbed and non-sorbed tracers through a fracture in crystalline rock, Radioact. Waste Management Nucl. Fuel Cycle, 4(2), 129-158, 1983.

Hoopes, J.A. and D.R.F. Harleman, Wastewater rechange and dispersion in porous media, J. Hydraul. Div. Am. Soc. Civ. Eng., 93(HY5), 51-71, 1967.

Iwai, K., Fundamental studies of fluid flow through a single fracture, Ph.D. dissertation, 208 pp., Univ. of Calif., Berkeley, 1976.

Klockars, C.-E., O. Persson and O. Landström, The hydraulic properties of fracture zones and tracer tests with non-reactive elements in Studsvik, KBS Nuclear Fuel Safety Project, Tech. Rep. 82-10, Stockholm, Sweden, 1982.

Lapidus, L. and N.R. Amundson, Mathematics of adsorption in beds: VI The effect of longitudinal diffusion on ion exchange and chromatographic columns, J. Phys. Chem., Ithaca, 56, 984-988, 1952.

Legrand-Marcq, C. and H. Laudelout, Longitudinal dispersion in a forest stream, J. Hydrol., 78, 317-324, 1985.

Levenspiel, O., Chemical Reaction Engineering, 2nd ed. John Wiley, New York, 1972.

Maini, Y.N.T., In situ hydraulic parameters in jointed rock - Their measurement and interpretation, Ph.D. dissertation, 320 pp., University of London, Imperial College, 1971.

Maloszewski, P. and A. Zuber, On the theory of tracer experiments in fissured rocks with a porous matrix, J. Hydrol., 79, 333-358, 1985.

Matheron, G. and G. de Marsily, Is transport in porous media always diffusive? A counter example, Water Resour. Res., 16(5), 901-917, 1980.

Moreno, L., I. Neretnieks and T. Eriksen, Analysis of some laboratory tracer runs in natural fractures, Water Resour. Res., 21(7), 951-958, 1985.

Muskat, M., The Flow of Homogeneous Fluids through Porous Media, McGraw-Hill, New York, 763 pp., 1937.

Neretnieks, I., A note on fracture flow dispersion mechanisms in the ground, Water Resour. Res., 19(2), 364-370, 1983.

Neretnieks, I., T. Eriksen and P. Tähtinen, Tracer movement in a single fissure in granitic rock: Some experimental results and their interpretation, Water Resour. Res., 18(4), 849-858, 1982.

Nordin, C.F., Jr. and B.M. Troutman, Longitudinal dispersion in rivers: The persistence of skewness in observed data, Water Resour. Res., 16(1), 123-128, 1980.

Novakowski, K.S., G.V. Evans, D.A. Lever and K.G. Raven, A field example of measuring hydrodynamic dispersion in a single fracture, Water Resour. Res., 21(8), 1165-1174, 1985a.

Novakowski, K.S., P.A. Flavelle, K.G. Raven and E.L. Cooper, Determination of groundwater flow pathways in fractured plutonic rock using a radioactive tracer, Int. J. Appl. Radiat. Isot., 36(5), 399-404, 1985b.

Pedersen, F.B., Prediction of longitudinal dispersion in natural streams, Ser. Pap. 14, Inst. of Hydrodyn. and Hydraul. Eng., Tech. Univ. of Denmark, Copenhagen, 1977.

Pickens, J.F. and G.E. Grisak, Scale-dependent dispersion in a stratified granular aquifer, Water Resour. Res., 17(4), 1191-1211, 1981.

Plummer, L.N., B.F. Jones and A.H. Truesdell, WATEQF - A Fortran IV version of WATEQ, a computer program for calculating chemical equilibrium of natural waters, U.S. Geol. Surv., Water Resources Investigations Report 76-13, 1976.

Raven, K.G. and K.S. Novakowski, Field investigations of solute transport properties of fractures in monzonitic gneiss, in Proceedings of the International Groundwater Symposium on Groundwater Resources Utilization and Contaminant Hydrogeology, vol. 2, pp. 507-516, International Association of Hydrogeologists, Montreal, Que., 1984.

Sauty, J.-P., An analysis of hydrodispersive transfer in aquifers, Water Resour. Res., 16(1), 145-158, 1980.

Sayre, W.W., Dispersion of mass in open-channel flow, Hydraul. Pap. 3, 73 pp., Colo. State Univ., Fort Collins, 1968.

Schlichting, H., Boundary-Layer Theory, 6th Ed., McGraw-Hill, New York, pp. 67-68, 1968.

Skagius, K. and I. Neretnieks, Porosities and diffusivities of some non-sorbing species in crystalline rocks, Water Resour. Res., 22(3), 389-398, 1986.

Taylor, G.I., The dispersion of matter in a solvent flowing slowly through a tube, Proc. R. Soc. London Ser. A, 219, 189-203, 1953.

Taylor, G.I., The dispersion of matter in turbulent flow through a pipe, Proc. R. Soc. London Ser. A, 223, 446-468, 1954.

Thackston, E.L. and P.A. Krenkel, Longitudinal mixing in natural streams, J. Sanit. Eng. Div. Am. Soc. Civ. Eng., 93(SA5), 67-90, 1967.

Tsang, Y.W. and C.F. Tsang, Channel model of flow through fractured media, Water Resour. Res., 23(3), 467-479, 1987.

Turner, G.A., The flow structure in packed peds, Chem. Eng. Sci., 7, 156-165, 1958.

Valentine, E.M. and I.R. Wood, Experiments in longitudinal dispersion with dead zones, J. Hydraul. Div. Am. Soc. Civ. Eng., 105(HY8), 999-1016, 1979.

Van Dyke, M., An Album of Fluid Motion, Parabolic Press, Stanford, Ca., 1982.

Van Genuchten, M.Th. and P.J. Wierenga, Mass transfer studies in sorbing porous media, I. Analytical solutions, Soil Sci. Soc. Am. J., 40, 473-480, 1976.

Van Genuchten, M.Th. and P.J. Wierenga, Mass transfer studies in sorbing porous media: II. Experimental evaluation with tritium, Soil Sci. Soc. Am. J., 41(2), 272-278, 1977.

Van Swaaij, W.P.M., J.C. Charpentier and J. Villermaux, Residence time distribution in the liquid phase of trickle flow in packed columns, Chem. Eng. Sci., 24, 1083-1095, 1969.

Villermaux, J. and W.P.M. Van Swaaij, Modèle représentatif de la distribution des temps de séjour dans un réacteur semi-infini à dispersion axiale avec zones stagnantes. Application a l'écoulement ruisselant dans des colonnes d'anneaux Raschig, Chem. Eng. Sci., 24, 1097-1111, 1969.

List of Figures

Figure 9. The field RTDs of tracer test no. 4 as determined from the borehole gamma detector and from groundwater samples with the best fit AD and ADTS model simulations.

Figure 10. The field RTDs of tracer test no. 5 as determined from groundwater samples with recirculation and without recirculation effects. Also shown is the best fit AD model simulation to the field RTD without recirculation effects.

Figure 11. The variation of mean mass transfer coefficient, $\bar{K}$, with mean fluid velocity, $\bar{v}$ determined from best fit of the ADTS model simulations.

Figure 12. The variation of longitudinal dispersivity, α_L, with mean fluid velocity, $\bar{v}$, determined from best fits of the AD and ADTS model simulations.

Table 1

Parallel-Plate Openings Determined from Hydraulic Tests
2b in μm

Activation Borehole	Observation Borehole						
	FS-5	FS-6	FS-10	FS-11	FS-13	FS-15	FS-16
FS-5	35	-	-	-	-	-	-
FS-6	-	140	120	110	100	145	135
FS-10	-	-	15	-	-	-	-
FS-11	-	141	190	190	150	140	-
FS-13	-	-	-	-	96	-	-
FS-15	-	110	-	124	-	145	-
FS-16	-	-	-	-	-	-	42

Table 2
Summary of Tracer Test Conditions

Test	Tracer	Test Boreholes		Flow Field	Borehole Spacing, m	M_{inj}	Q $L.h^{-1}$	ΔH m
		Injection	Withdrawal					
1	^{82}Br	FS-6	FS-15	Inj.-With.	12.7	27 MBq	30.0	4.60
2	Na Fl.	FS-15	FS-6	Inj.-With.	12.7	100 mg	32.0	4.90
3	^{82}Br	FS-6	FS-15	Rad.-Conv.	12.7	27 MBq	14.0	0.70
4	^{82}Br	FS-6	FS-15	Inj.-With.	12.7	40 MBq	36.6	2.35
5	^{82}Br	FS-6	FS-11	Inj.-With.	29.8	40 MBq	36.6	5.95

Table 3
Characteristics of the Fracture RTD Curves

Test	t_p h	C_p	E_p h^{-1}	Final C/C_p	m_{rec}
1	3.5	30.5 KBq.L^{-1}	0.034	0.24	0.45
2	2.5	140 µg.L^{-1}	0.045	0.24	0.50
3	20.5	28.6 KBq.L^{-1}	0.015	0.44	0.55
4	5.5	94.0 KBq.L^{-1}	0.086	0.29	0.65
5*	97.0	7.0 KBq.L^{-1}	0.0064	0.85	-
5+	67.0	5.9 KBq.L^{-1}	0.0054	0.47	0.55

* with recirculation effect

+ without recirculation effect

Table 4
Summary of Best Fit AD and ADTS Model Parameters

	AD Model Parameters			ADTS Model Parameters			
Test	2b μm	α_L m	ζ	2b μm	α_L m	N	ϕ
1	90	.95	1.24	90	.95	1.4	0.45
2	105	1.0	1.10	105	1.0	1.6	0.35
3	95	3.0	1.14	95	3.0	0.8	0.65
4	115	1.0	1.21	115	1.0	1.0	0.65
5	45	6.3	0.70	45	6.3	0.0	1.00

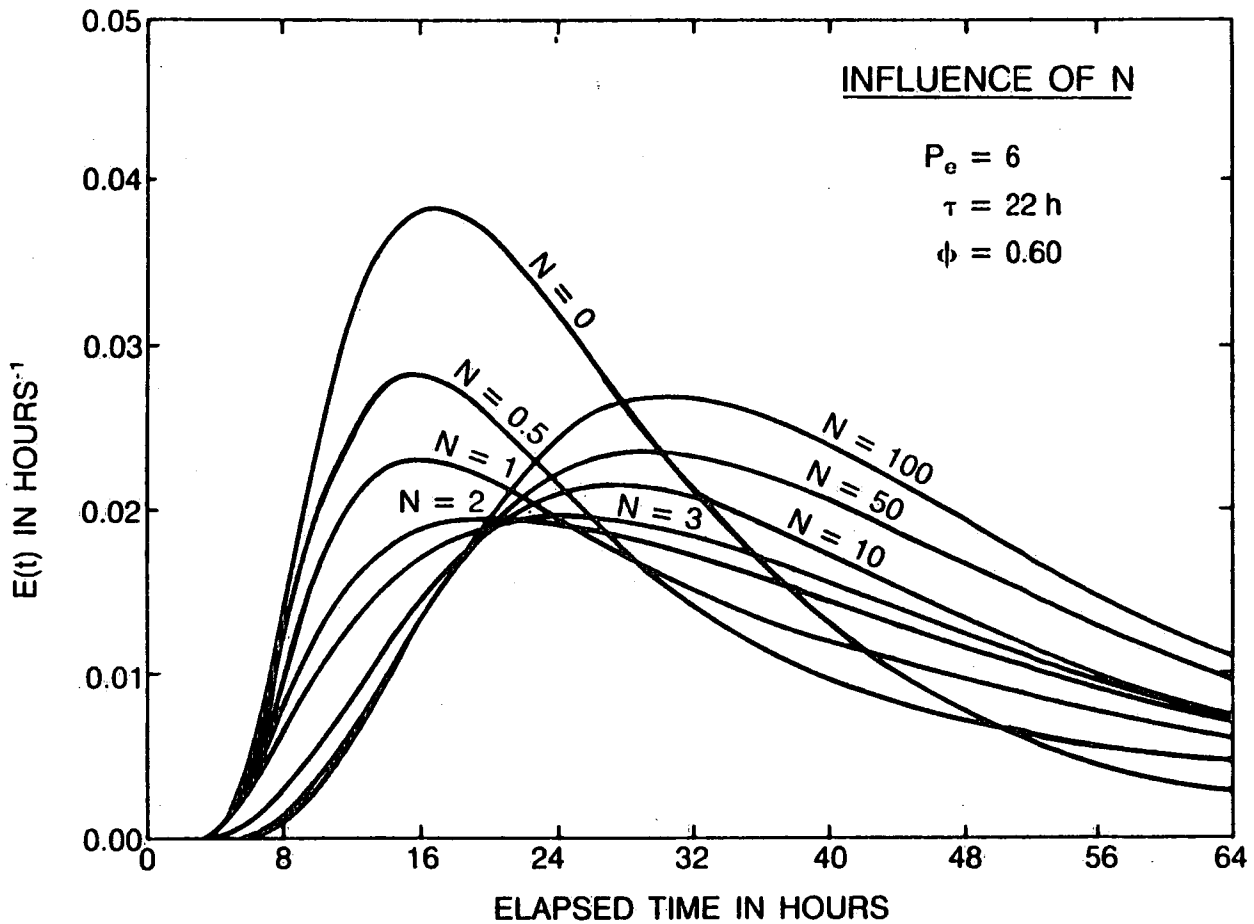
INFLUENCE OF N
P_e = 6
τ = 22 h
ϕ = 0.60
N = 0
N = 0.5
N = 1
N = 2
N = 3
N = 10
N = 50
N = 100
E(t) IN HOURS^{-1}
0.05
0.04
0.03
0.02
0.01
0.00
0
8
16
24
32
40
48
56
64
ELAPSED TIME IN HOURS

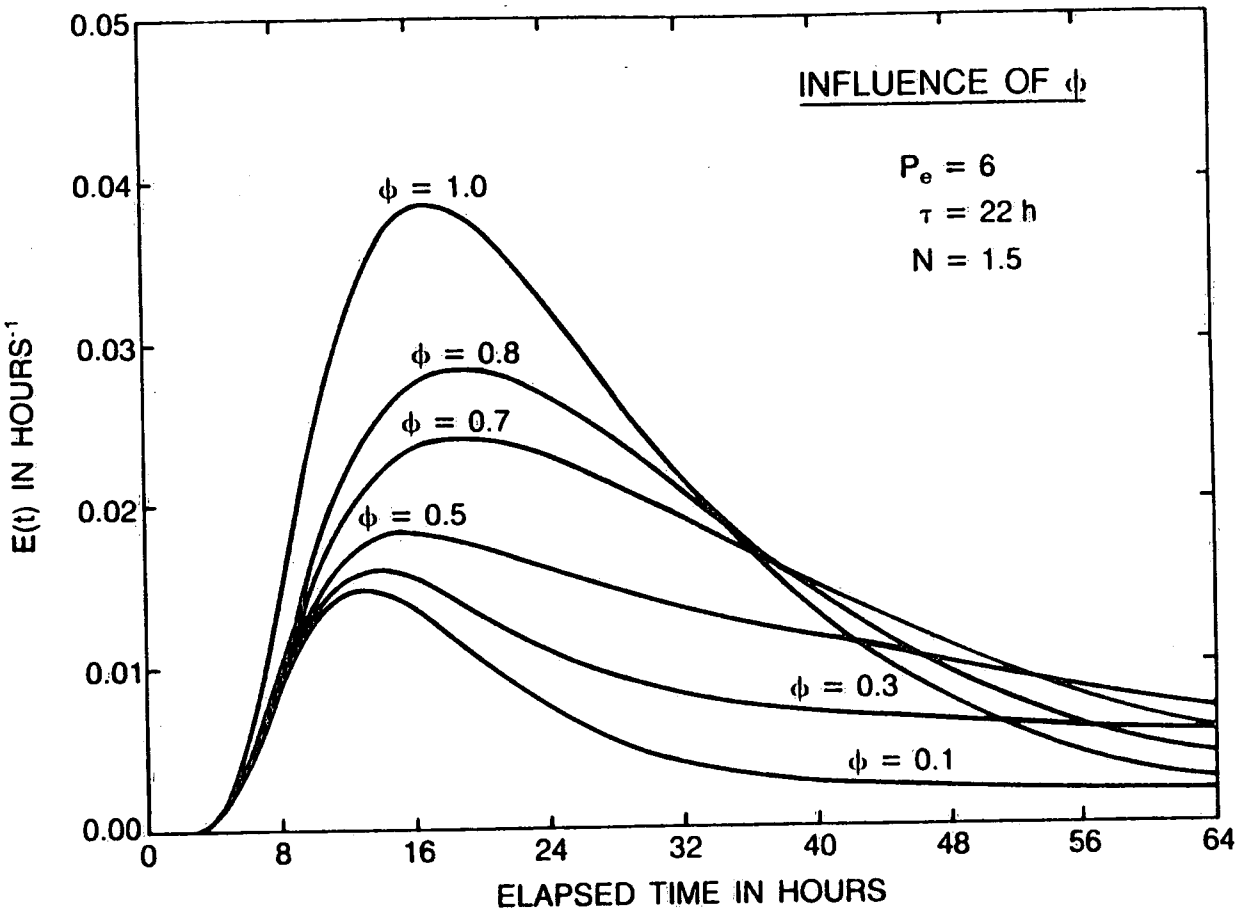
INFLUENCE OF ϕ
P_e = 6
τ = 22 h
N = 1.5
ϕ = 1.0
ϕ = 0.8
ϕ = 0.7
ϕ = 0.5
ϕ = 0.3
ϕ = 0.1
E(t) IN HOURS^{-1}
0.05
0.04
0.03
0.02
0.01
0.00
0
8
16
24
32
40
48
56
64
ELAPSED TIME IN HOURS

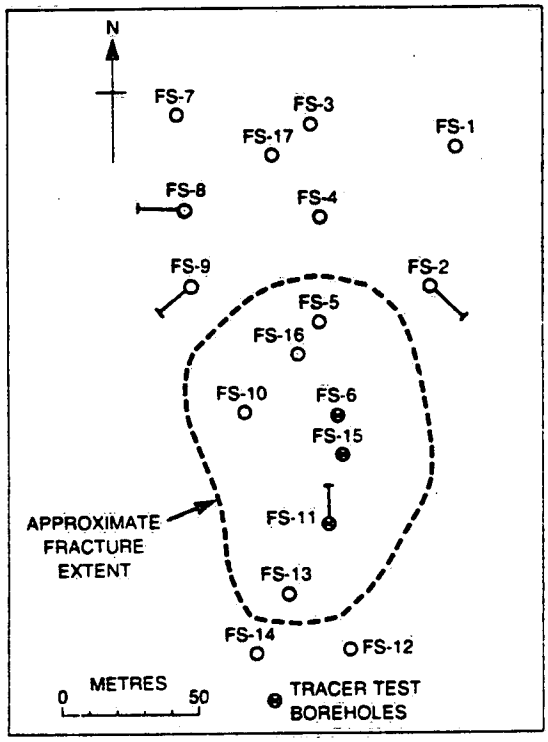
N
FS-7
FS-3
FS-17
FS-1
FS-8
FS-4
FS-9
FS-2
FS-5
FS-16
FS-10
FS-6
FS-15
APPROXIMATE
FRACTURE
EXTENT
FS-11
FS-13
FS-14
FS-12
0
METRES
50
TRACER TEST
BOREHOLES

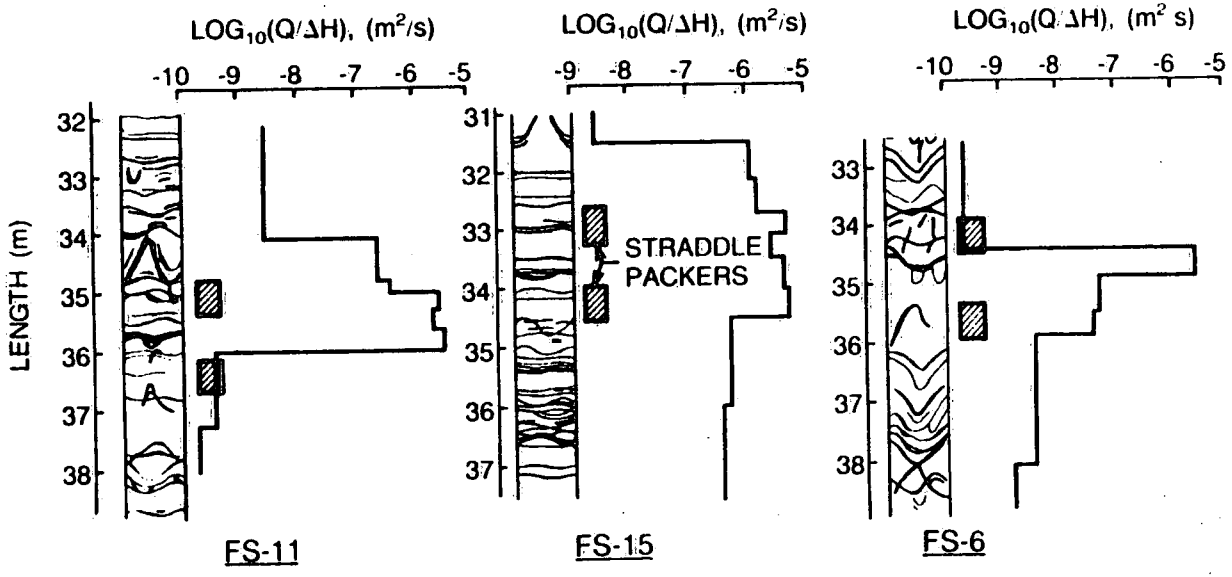
LOG10(Q/ΔH), (m²/s)
-10 -9 -8 -7 -6 -5
LENGTH (m)
32
33
34
35
36
37
38
FS-11
LOG10(Q/ΔH), (m²/s)
-9 -8 -7 -6 -5
31
32
33
34
35
36
37
STRADDLE PACKERS
FS-15
LOG10(Q/ΔH), (m² s)
-10 -9 -8 -7 -6 -5
33
34
35
36
37
38
FS-6

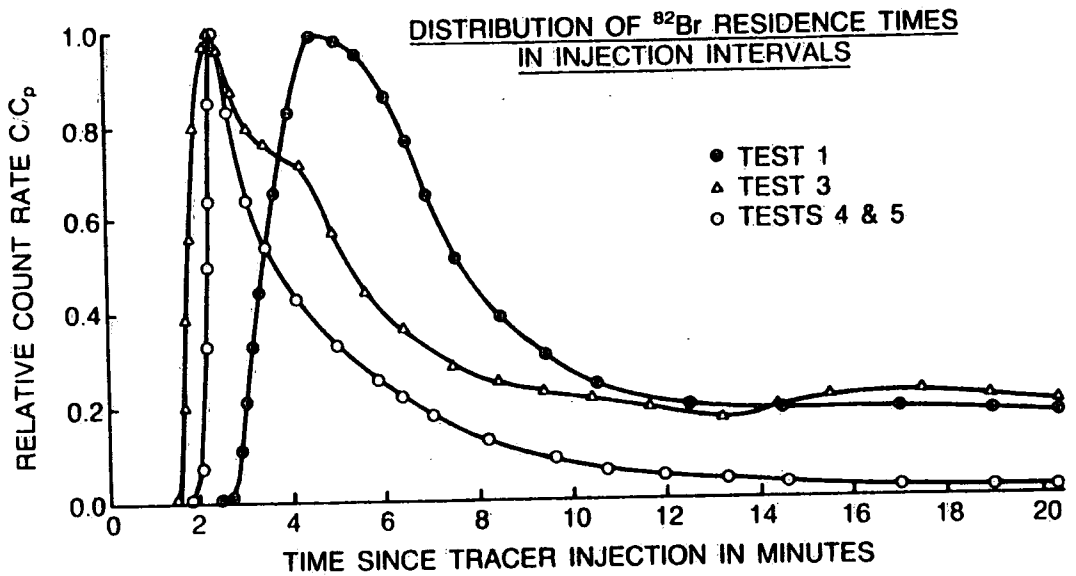
DISTRIBUTION OF ^{82}Br RESIDENCE TIMES
IN INJECTION INTERVALS
TEST 1
TEST 3
TESTS 4 & 5
RELATIVE COUNT RATE C/C$_p$
1.0
0.8
0.6
0.4
0.2
0.0
0
2
4
6
8
10
12
14
16
18
20
TIME SINCE TRACER INJECTION IN MINUTES

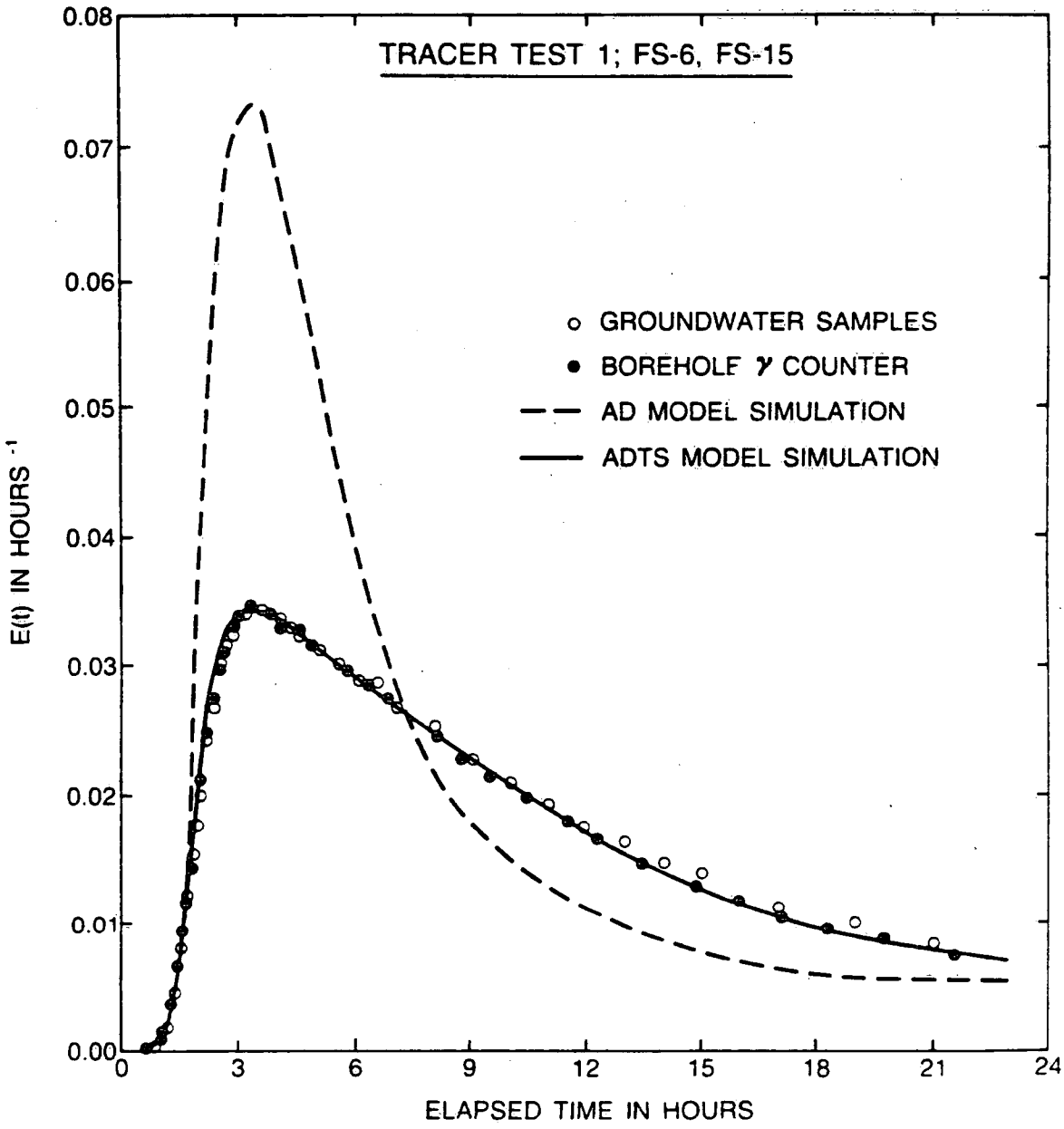
TRACER TEST 1; FS-6, FS-15
GROUNDWATER SAMPLES
BOREHOLE γ COUNTER
AD MODEL SIMULATION
ADTS MODEL SIMULATION
E(t) IN HOURS⁻¹
0.08
0.07
0.06
0.05
0.04
0.03
0.02
0.01
0.00
0
3
6
9
12
15
18
21
24
ELAPSED TIME IN HOURS

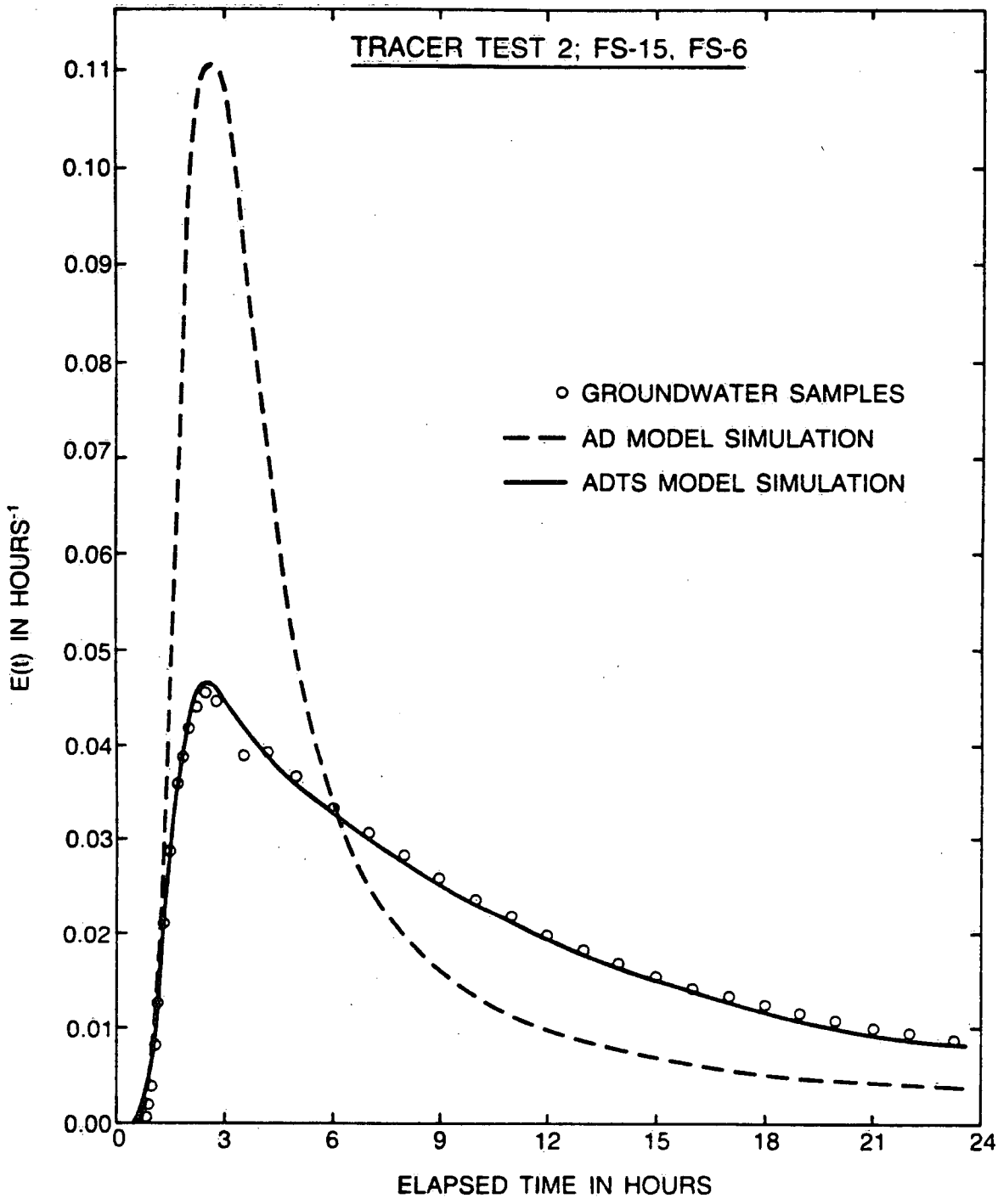
TRACER TEST 2; FS-15, FS-6
GROUNDWATER SAMPLES
AD MODEL SIMULATION
ADTS MODEL SIMULATION
E(t) IN HOURS^{-1}
0.11
0.10
0.09
0.08
0.07
0.06
0.05
0.04
0.03
0.02
0.01
0.00
0
3
6
9
12
15
18
21
24
ELAPSED TIME IN HOURS

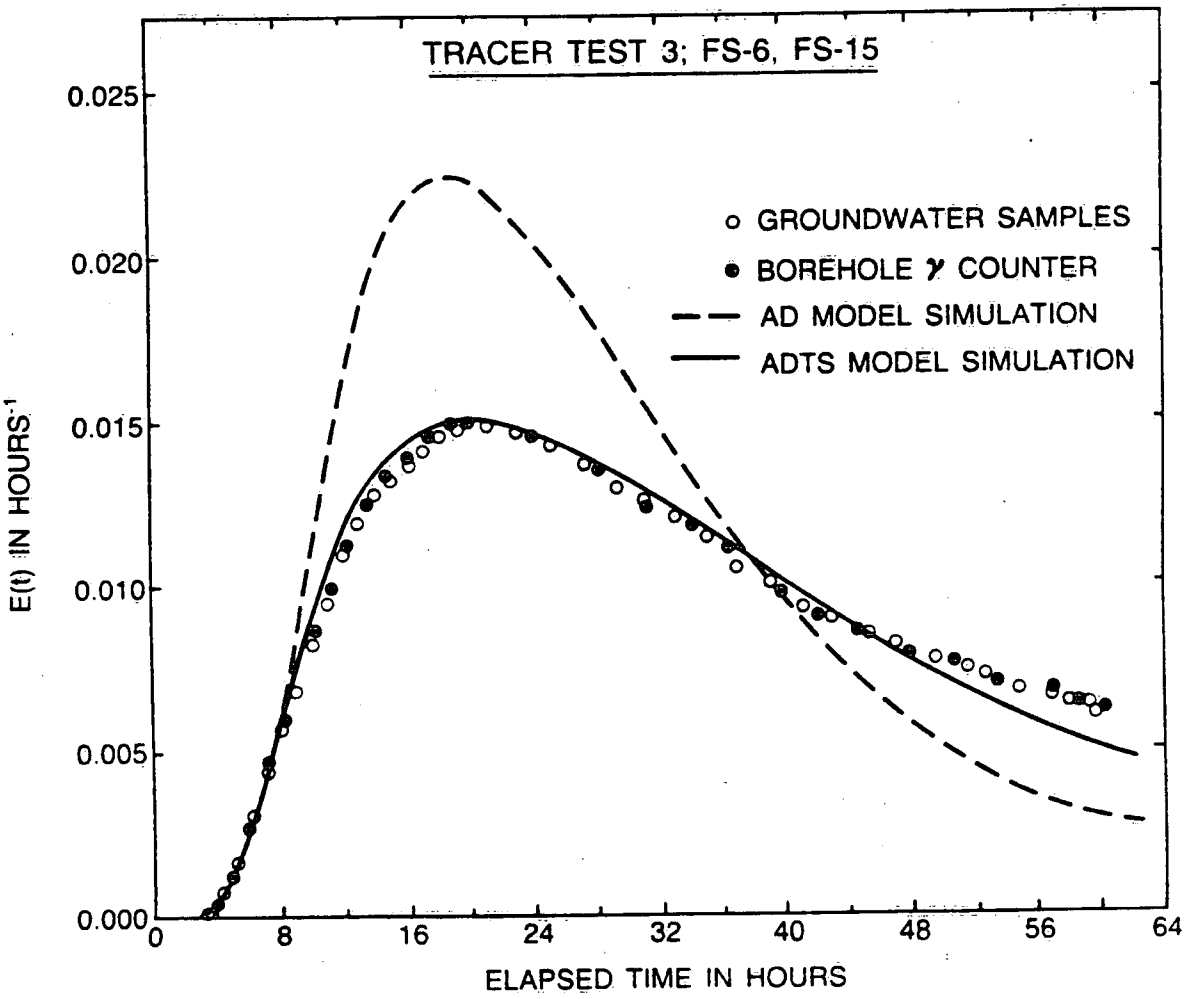
TRACER TEST 3; FS-6, FS-15
0.025
0.020
0.015
0.010
0.005
0.000
E(t) IN HOURS^{-1}
0
8
16
24
32
40
48
56
64
ELAPSED TIME IN HOURS
GROUNDWATER SAMPLES
BOREHOLE γ COUNTER
AD MODEL SIMULATION
ADTS MODEL SIMULATION

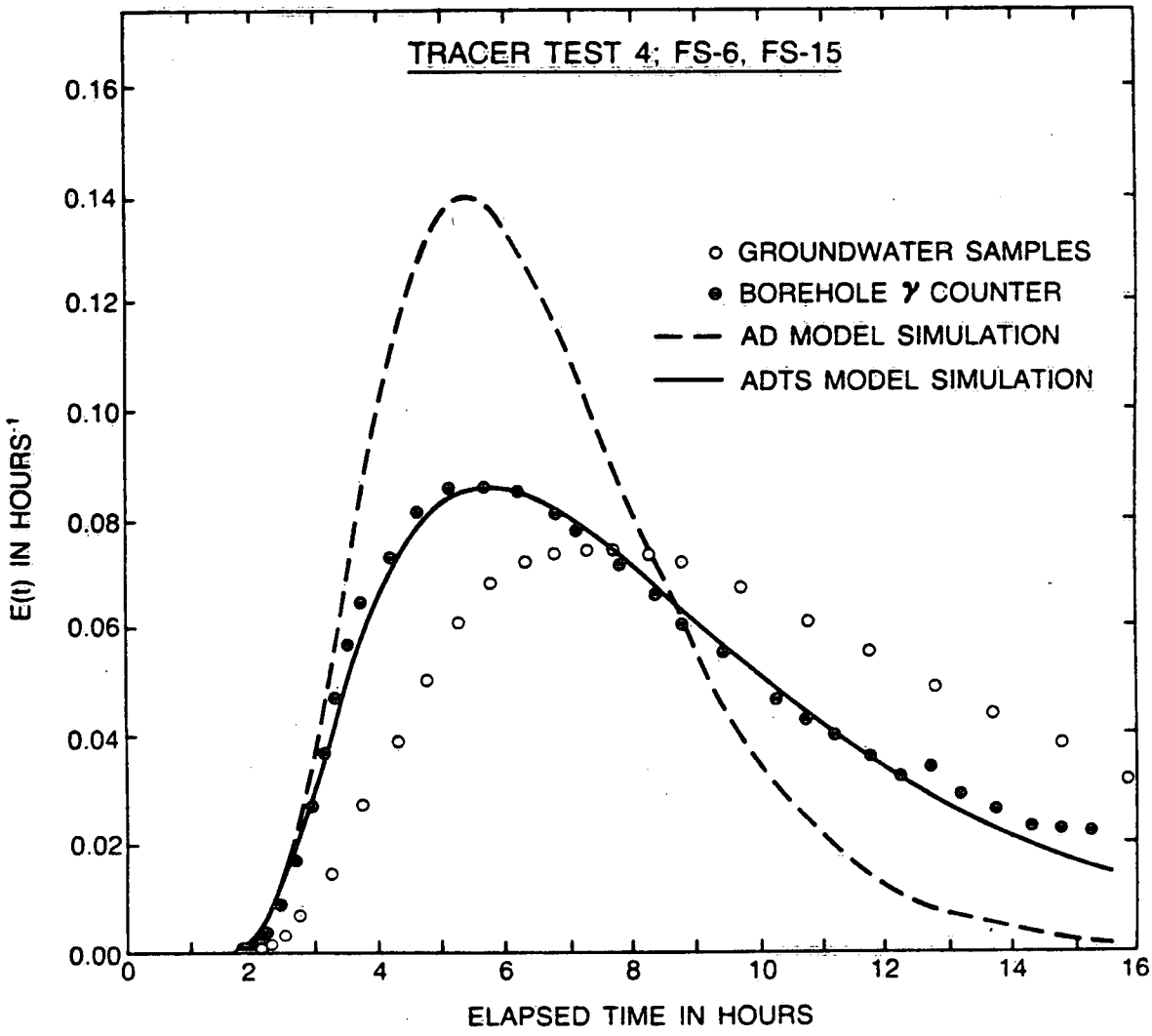
TRACER TEST 4; FS-6, FS-15
GROUNDWATER SAMPLES
BOREHOLE γ COUNTER
AD MODEL SIMULATION
ADTS MODEL SIMULATION
E(t) IN HOURS⁻¹
0.16
0.14
0.12
0.10
0.08
0.06
0.04
0.02
0.00
0
2
4
6
8
10
12
14
16
ELAPSED TIME IN HOURS

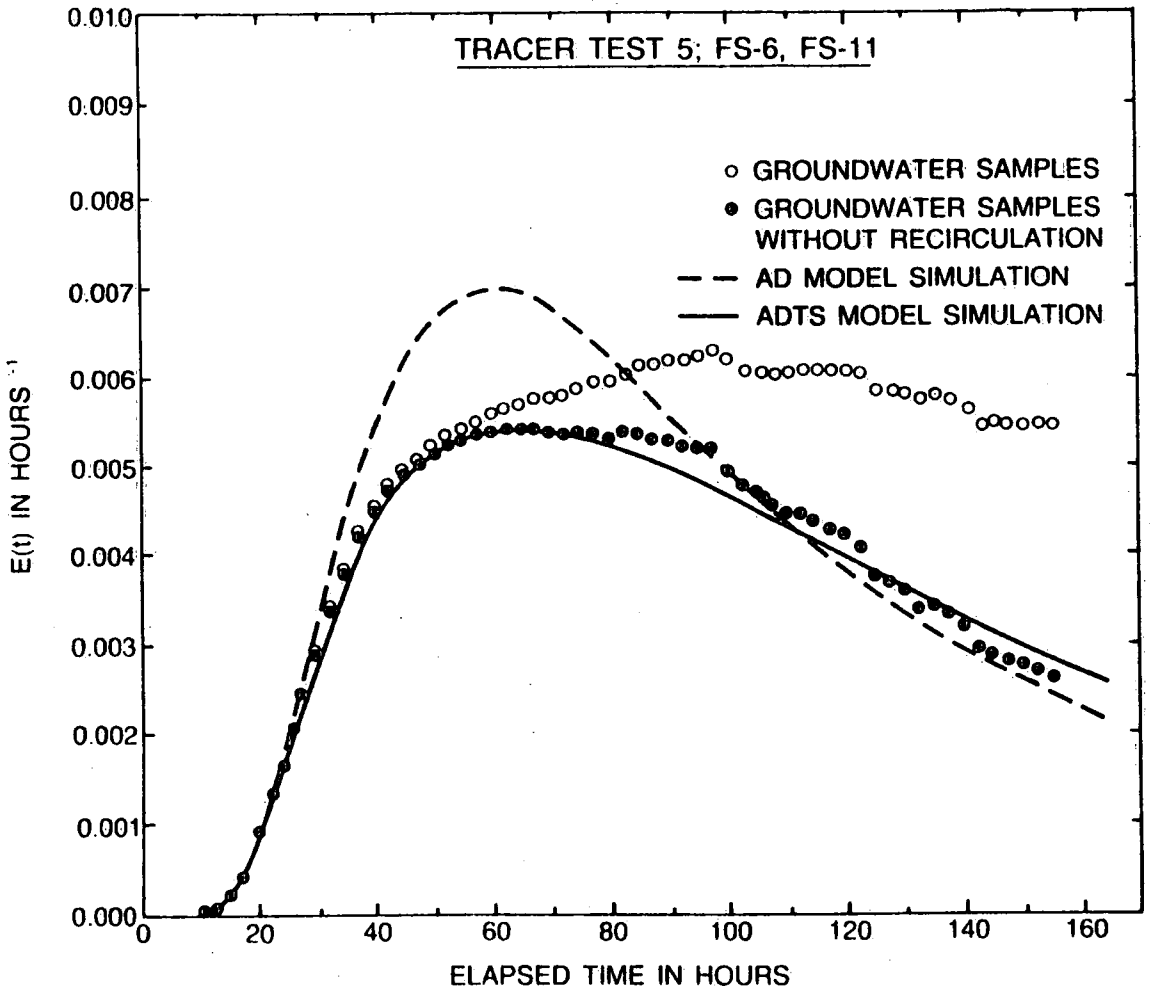
TRACER TEST 5; FS-6, FS-11
GROUNDWATER SAMPLES
GROUNDWATER SAMPLES WITHOUT RECIRCULATION
AD MODEL SIMULATION
ADTS MODEL SIMULATION
E(t) IN HOURS⁻¹
0.010
0.009
0.008
0.007
0.006
0.005
0.004
0.003
0.002
0.001
0.000
0
20
40
60
80
100
120
140
160
ELAPSED TIME IN HOURS

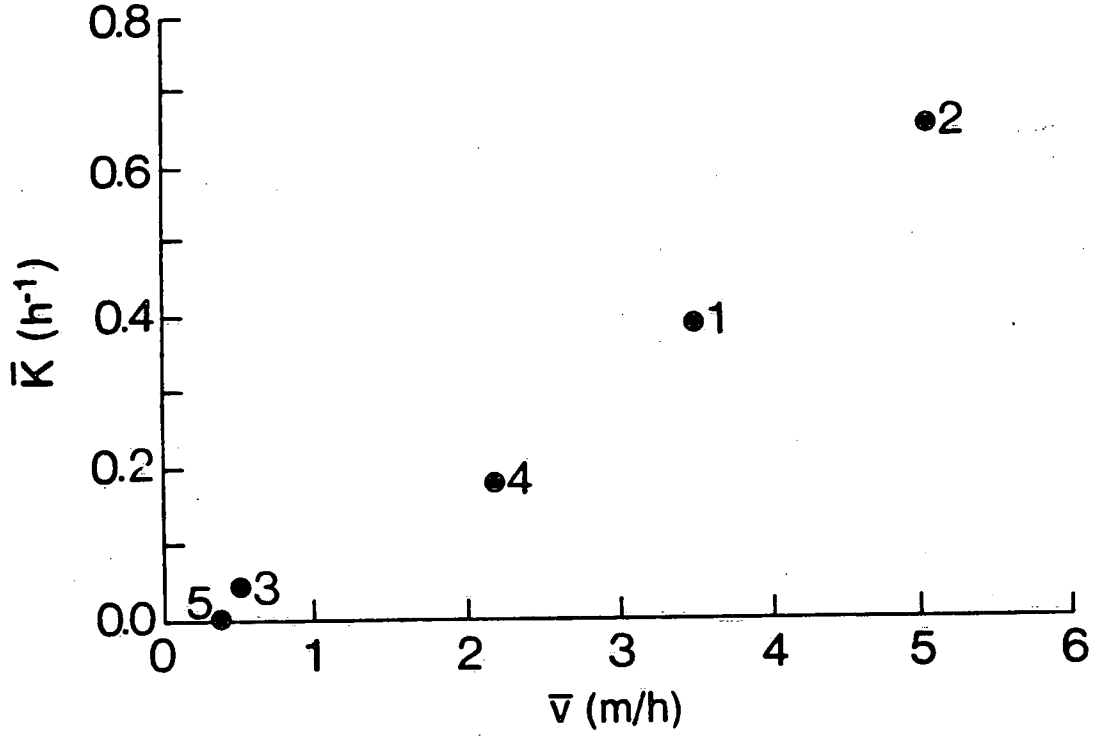
0.8
0.6
0.4
0.2
0.0
$\bar{K}$ (h^{-1})
0
1
2
3
4
5
6
$\bar{v}$ (m/h)
1
2
3
4
5

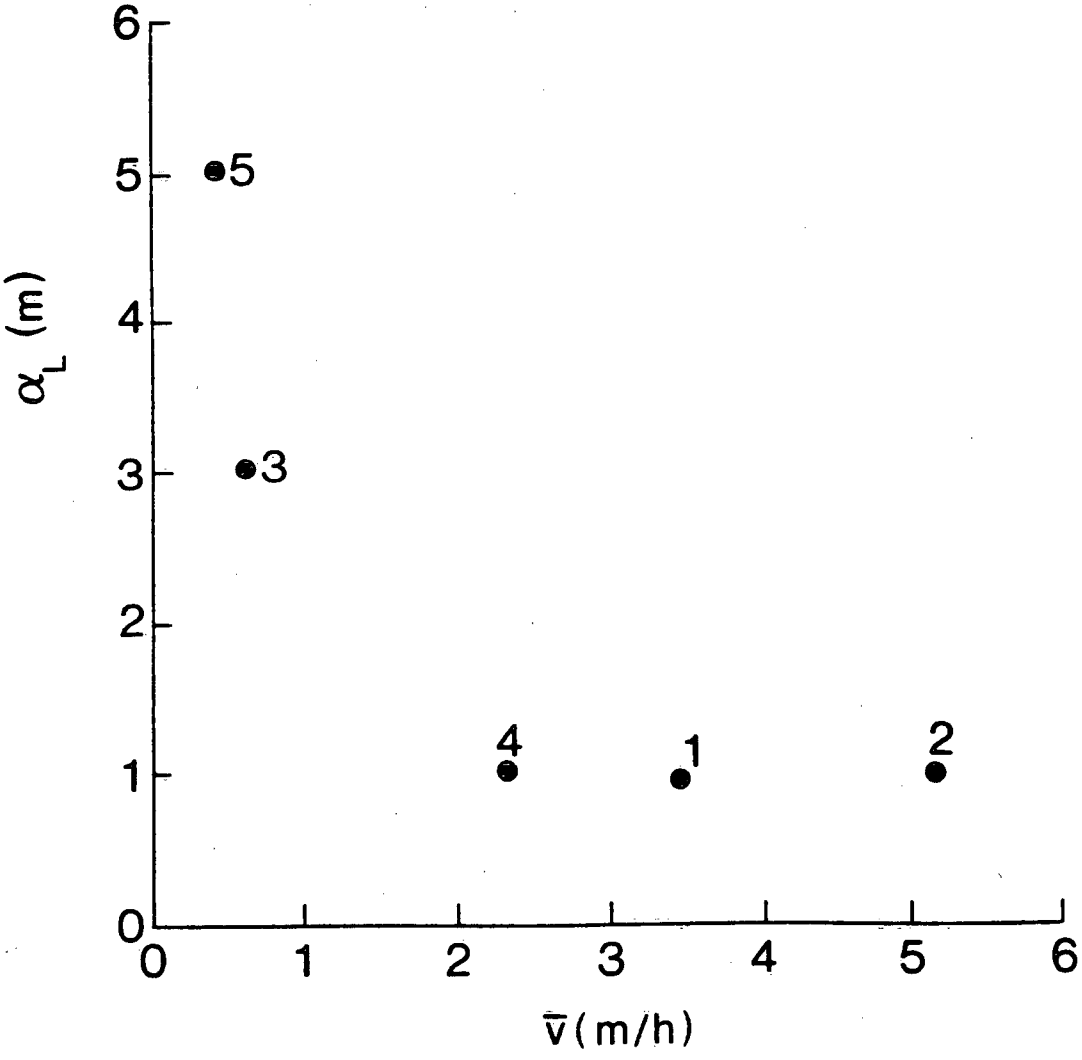
6
5
4
3
2
1
0
α_L (m)
0
1
2
3
4
5
6
$\bar{v}$ (m/h)
1
2
3
4
5